OPTIMAL LOW THRUST, THREE BURN ORBIT TRANSFERS WITH LARGE PLANE CHANGES

Thesis by

Keith Peter Zondervan

In Partial Fulfillment of the Requirements

for the Degree of

Doctor of Philosophy

California Institute of Technology

Pasadena, California

1983

(Submitted May 16, 1983)

ACKNOWLEDGEMENTS

The creation of this thesis would not have been possible without the generous support of The Aerospace Corporation. In addition to financial support, Aerospace also provided me with many other resources: the library, computer system, and intellect of my colleagues - to name just a few. Special thanks go especially to Dr. John T. Betts and Mr. Richard G. Stern for their generous guidance and assistance and to Mary Ann Ford for typing this manuscript.

Special thanks are also expressed to two Caltech faculty members - Dr. Thomas K. Caughey, my advisor, and Dr. Lincoln J. Wood. Their encouragement and guidance in the preparation of this thesis is much appreciated.

The love and support shown me by my family deserves more thanks than I can give. My parents instilled me with my sense of values and love of learning. My twin brother, Kevin, through brotherly competition, provided me with the incentive to always try to do my best. My wife, Barbara, made the many long hours spent working on this thesis endurable, through her patience, helpfulness, and love.

The motto of Caltech, first spoken 2000 years ago by Jesus Christ states: The Truth Shall Make You Free. This thesis is dedicated to the revelation of His Truth.

ABSTRACT

During the last twenty-five years, much attention has been devoted to the problem of optimal orbit transfer. The problem has been conveniently divided into two categories - unlimited thrust (or acceleration) orbit transfers and limited thrust (or acceleration) orbit transfers. The unlimited thrust orbit transfers use infinite thrust, zero burn time burns and hence have also come to be known as impulsive burn orbit transfers. In general it has been found that optimal (i.e., minimum fuel, time-free) solutions to these types of transfers require two or possibly three burns. The limited thrust transfers, in contrast, do not use impulsive burns but use burns which have a finite thrust level and a nonzero burn time and, hence, are also known as finite burn orbit transfers.

If our attention is restricted to finite multi-burn transfers which have burn times less than an orbital period, two classes of transfers emerge. These classes of transfers are either Geometrically Similar to the 2-Burn Impulsive (GS2BI) transfers or Geometrically Similar to the 3-Burn Impulsive (GS3BI) transfers. For example, if a 2-burn impulsive solution has a perigee burn followed by an apogee burn, the GS2BI finite burn transfer would use one or more perigee burns followed by one or more apogee burns.

Recent studies have presented optimal solutions to GS2BI finite burn orbit transfers for various thrust to weight ratios. The current study presents the optimal solutions to GS3BI finite burn orbit transfers between a 28.5° inclined low-earth orbit and a series of 63.4° inclined circular orbits and a series of 63.4° inclined elliptical orbits with twelve hour periods. Also presented are optimal solutions to GS3BI finite burn orbit transfers between 97° inclined high-earth orbits and a 57° inclined low-earth orbit. Optimal solutions are found to be bounded by a lower limit on the initial thrust to weight ratio. It is shown that as the final perigee altitude is increased, the GS3BI finite burn transfer degenerates to a GS2BI finite burn transfer much as it would for the impulsive case.

Analysis of the optimal steering during various burns reveals a natural division of the steering strategies into two categories based on whether a burn results in a predominant change in the orbit size or the orbit plane. The similarity of these optimal steering strategies to previously obtained simple "near-optimal" steering strategies is discussed.

TABLE OF CONTENTS

PAGE

LIST OF FIGURES

LIST OF TABLES

Chapter 1

INTRODUCTION

During the last twenty-five years, much attention has been devoted to the problem of optimal orbit transfer [1-15]. The problem has been conveniently divided into two categories - unlimited thrust (or acceleration) orbit transfers and limited thrust (or acceleration) orbit transfers. The unlimited thrust orbit transfers were shown by Lawden [2] to use infinite thrust, zero burn time burns and hence have also come to be known as impulsive burn orbit transfers. In general it has been found that optimal (i.e., minimum fuel time-free) solutions to these types of transfers require two or possibly three burns [3-5]. The limited thrust transfers, in contrast, do not use impulsive burns but use burns which have a finite thrust level and a nonzero burn time and, hence, are also known as finite burn orbit transfers.

Finite 1-burn solutions to the optimal orbit transfer problem are numerous in the literature [1, 2, 6-10]. More recently, finite multi-burn solutions which are Geometrically Similar to the 2-Burn Impulsive (GS2BI) solutions have also been obtained [11-13]. Typically, if a 2-burn impulsive solution has a perigee burn followed by an apogee burn, these GS2BI finite burn transfers have one or more perigee burns followed by one or more apogee burns. This thesis is devoted to the obtainment and characterization of finite 3-burn solutions to the optimal orbit transfer problem which are Geometrically Similar to the 3-Burn Impulsive (GS3BI) solutions.

The finite multi-burn orbit transfer problem is characterized by a thrust or acceleration level which is bounded by a zero lower level and a finite upper level. The first order necessary conditions for both thrust-limited and acceleration-limited optimal solutions are developed in Chapter 2 and show that an optimal orbit transfer should consist of one or more zero or null thrust (NT) arcs, intermediate thrust (IT) arcs, and/or maximum thrust (MT) arcs. A review of the literature on the optimality of IT arcs revealed, however, that it is not possible to join an IT arc to a NT or MT arc for the class of problem considered here. Thus, IT arcs will not exist for the orbit transfer problems considered in this study.

The techniques used to solve optimization problems have typically been divided into two types - direct methods and indirect methods. Direct methods minimize (or maximize) the performance index directly by making appropriate changes to the input variables. Problems utilizing this type of method are often referred to as nonlinear programming (NLP) or parameter optimization problems. Indirect methods accomplish the optimization task by employing the requirement that the first variation of the performance index must be zero at the solution. The solution of the resulting first order necessary conditions for optimal control problems usually involves solving a two-point boundary value problem (TPBVP). Chapter 3 examines these methods and discusses the approach taken by Hersom, et al. [11] of combining both the direct and indirect methods to form a hybrid method. The basic difference between the hybrid and indirect methods is the satisfaction of transversality conditions implicitly rather than explicitly. This advantage, among others, makes the hybrid method a particularly attractive choice for solving optimal control problems.

Chapter 4 presents the optimal solutions to GS3BI finite burn orbit transfers between a 28.5° inclined low-earth orbit and a series of 63.4° inclined circular orbits as well as a series of 63.4° inclined elliptical orbits with twelve hour periods. Also presented are optimal solutions to GS3BI finite burn orbit transfers between 97° inclined high-earth orbits and a 57° inclined low-earth orbit. Thrust to weight ratios as low as .02 are considered. An analysis of the optimal steering during various burns is made in several coordinate frames in an attempt to discern its similarity to previously obtained simple "near-optimal" steering strategies [14-15].

Chapter 2

THE OPTIMAL CONTROL PROBLEM

2.1 COORDINATE SYSTEM DEFINITIONS

2.1.1. Earth Centered Inertial (ECI) Coordinate System

The ECI Coordinate System (also known as the Geocentric Equatorial coordinate system) is depicted in Figure 1. This coordinate system has its origin at the earth's center. The fundamental plane is the equator and the positive x-axis points in the vernal equinox direction, . The z-axis points in the direction of the north pole and the y-axis completes the right-handed system. Unless stated otherwise, this coordinate system will be assumed throughout the rest of this report.

Figure 1. The Earth Centered Inertial System

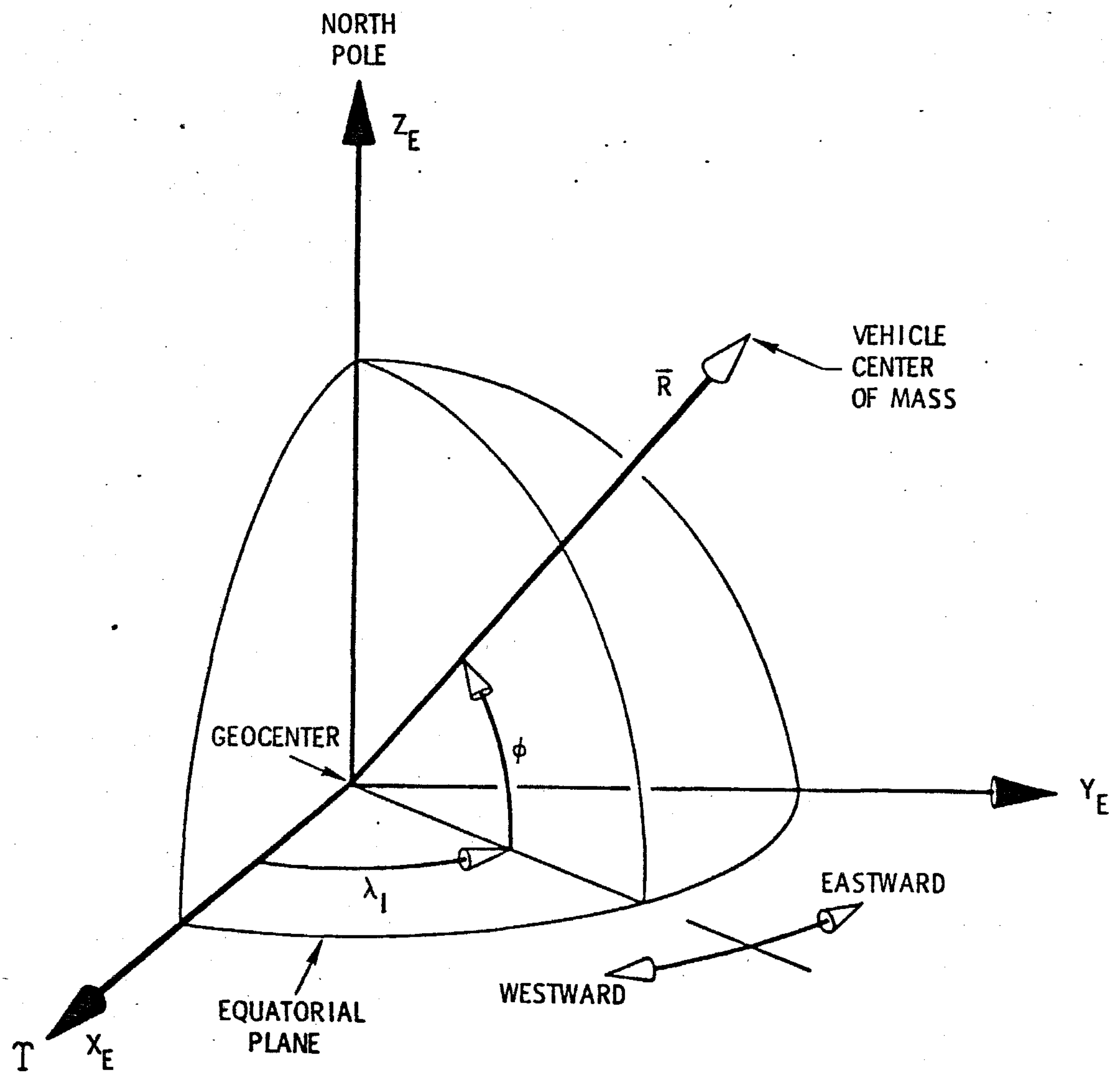

$\overline{R}$ VEHICLE POSITION

λ_I INERTIAL LONGITUDE

ϕ GEOCENTRIC LATITUDE

2.1.2 Orbit Plane Coordinate System

Assuming the earth is a sphere (and thus has a spherical earth gravity potential function), ballistic atmosphere-free trajectories about the earth define conic sections. Hence, the orbit plane coordinate system, where the fundamental plane is the plane of a coasting vehicle's orbit, is one of the most convenient coordinate frames for describing the motion of space vehicles. This frame and its relation to the ECI coordinate frame are depicted in Figure 2.

Five independent quantities called "orbital elements" are sufficient to completely describe the size, shape, and orientation of an orbit plane about a spherical earth. A sixth element is required to locate the vehicle along the orbit. The classical set of six orbital elements are defined with the help of Figures 2 and 3 as follows:

1. a, semi-major axis - half the maximum diameter of the conic-infinite for parabolic motion, positive for elliptical motion, and negative for hyperbolic motion.
2. e, eccentricity - a measure of the deviation of the conic from a circle-numerically zero for a circle, positive but less than one for an ellipse, equal to one for a parabola and greater than one for a hyperbola.
3. i, orbital inclination - the angle from the equatorial plane to the orbital plane, measured with positive rotation about the ascending node and in a plane normal to the ascending node.

Figure 2. Relation of Orbital Plane to ECI Coordinate System

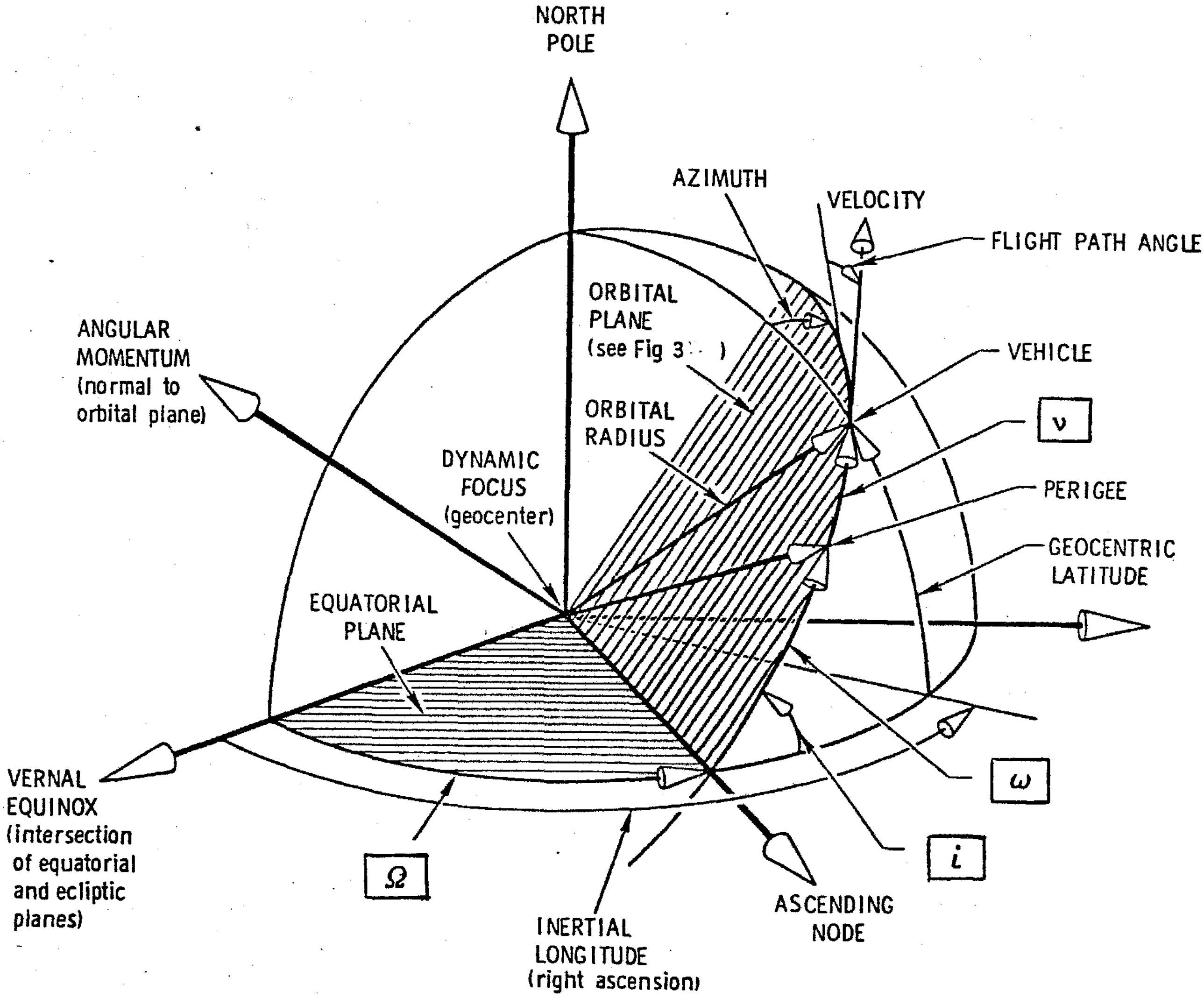

THE ILLUSTRATED ORBIT IS POSIGRADE

Figure 3. Elliptical Orbit Geometry

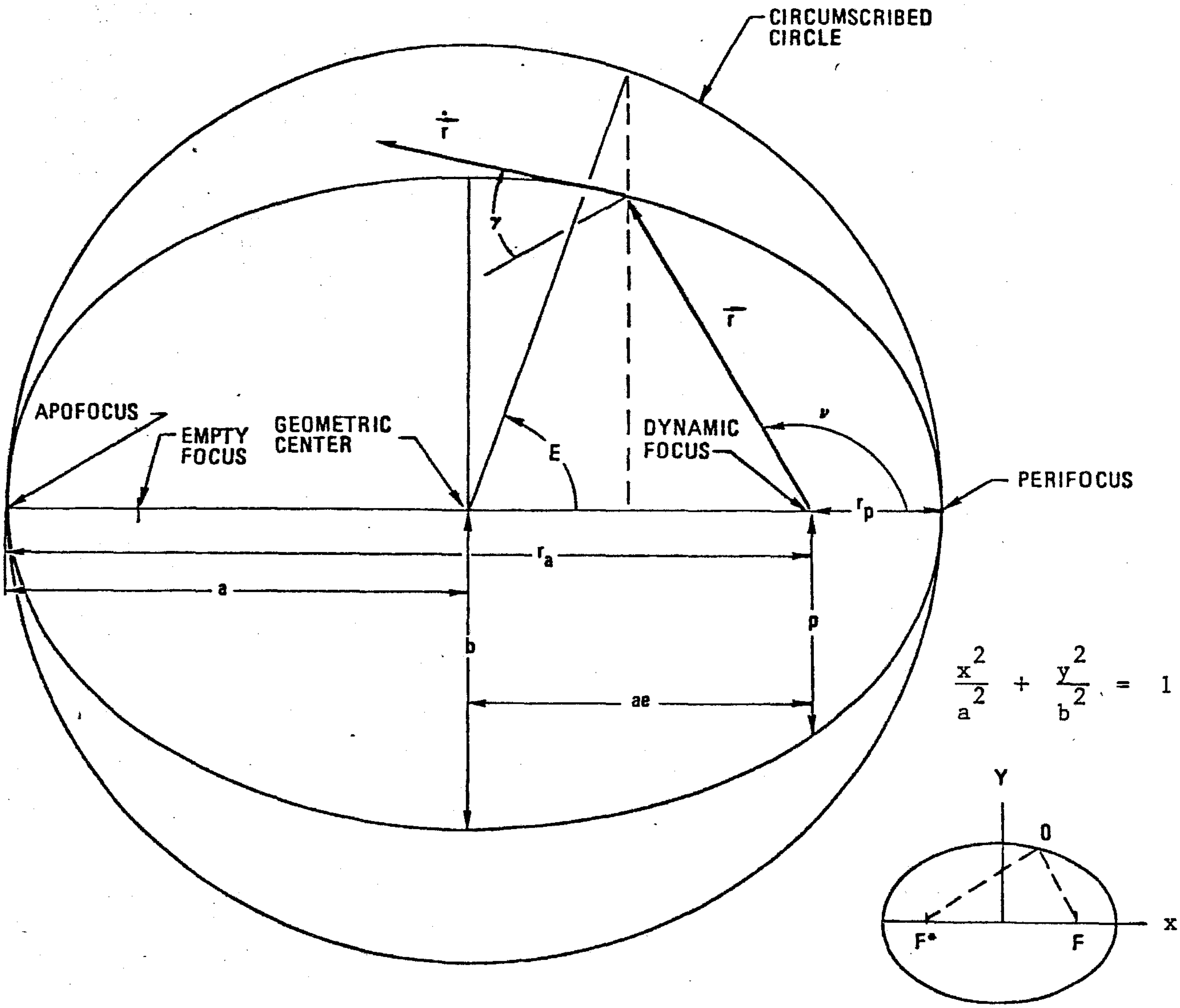

$$\frac{x^2}{a^2} + \frac{y^2}{b^2} = 1$$

a	SEMI-MAJOR AXIS
b	SEMI-MINOR AXIS
e	ECCENTRICITY
E	ECCENTRIC ANOMALY
p	SEMI-LATUS RECTUM
$\bar{r}$	POSITION
$\dot{\bar{r}}$	VELOCITY
r_a	APOFOCUS RADIUS
r_p	PERIFOCUS RADIUS
γ	FLIGHT PATH ANGLE
ν	TRUE ANOMALY

$OF^* + OF = 2a$

$0 < a < \infty$

$0 \leq e < 1$

$p = a\,(1-e^2)$

$\gamma > 0 \Longrightarrow 0 < \nu < 180^0$

$\gamma < 0 \Longrightarrow 180^0 < \nu < 360^0$

4. Ω , right ascension of the ascending node - the angle measured in the equatorial plane from a principal axis (normally the vernal equinox) to the orbit's ascending node (the line defining the intersection of the equatorial and orbital planes, directed from the origin to the point of passage of the vehicle traveling from the southern hemisphere towards the northern hemisphere).

5. ω, argument of perigee - the angle measured about a focus from the ascending node to the perifocus. (The perifocus is the point on the orbit having minimum radius).

6. ν , true anomaly - the angle, measured at the focus, subtended by the perifocus and the vehicle. (The true anomaly may be replaced as a classical orbital element by the eccentric anomaly, time relative to perifocal passage, or the argument of latitude, u, which is the sum of ω and ν .

In place of a and e, it is often more convenient to use apogee altitude, h_a, and perigee altitude, h_p. These quantities are defined with the help of Figure 3 as follows:

$$h_a = r_a - r_e$$

$$h_p = r_p - r_e$$

where r_e is the equatorial radius of the earth.

2.1.3 Inertial Velocity Local Horizontal (VIH) Coordinate System

Besides the ECI coordinate system, it will be convenient to represent the thrust vector of the vehicle in two other coordinate systems - the Inertial Velocity Local Horizontal (VIH) coordinate system and the Inertial Velocity (VI) coordinate system. The VIH coordinate system is depicted in Figure 4. It is a rotating system with its center at the vehicle center of mass. The fundamental plane is the geocentric local horizon (i.e., the plane normal to $\underline{r}$). The positive x-axis is directed along the azimuth of the inertial velocity vector and lies within the fundamental plane (i.e., the x-axis is the projection of $\dot{\underline{r}}$ in the fundamental plane). The z-axis is normal to the fundamental plane and is directed toward the geocenter. The y-axis lies in the fundamental plane and completes the right-handed system.

2.1.4 Inertial Velocity (VI) Coordinate System

The VI coordinate system will also be used to represent the thrust vector and is depicted in Figure 5. This system may be obtained from the VIH coordinate system by a rotation through the inertial flight path angle. The Fundamental plane is the instantaneous inertial trajectory plane (i.e., the orbital plane) and the positive x-axis points in the inertial velocity direction. The positive y-axis is normal to the fundamental plane and points in the $\dot{\underline{r}} \times \underline{r}$ direction. The z-axis lies in the fundamental plane and completes the right-handed system.

Figure 4. The Inertial Velocity Local Horizontal System

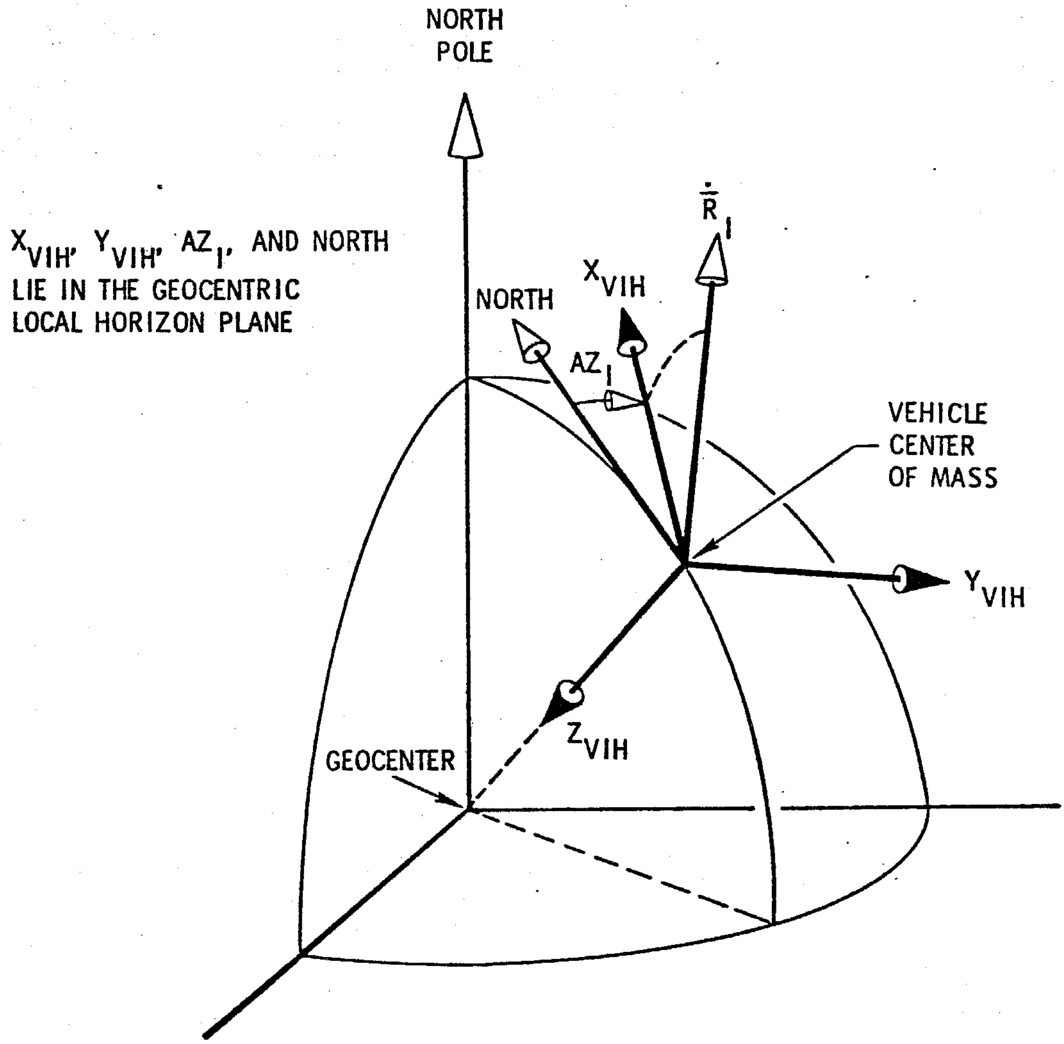

$\dot{\bar{R}}_I$ INERTIAL VELOCITY

AZ_I INERTIAL AZIMUTH

Figure 5. The Inertial Velocity System

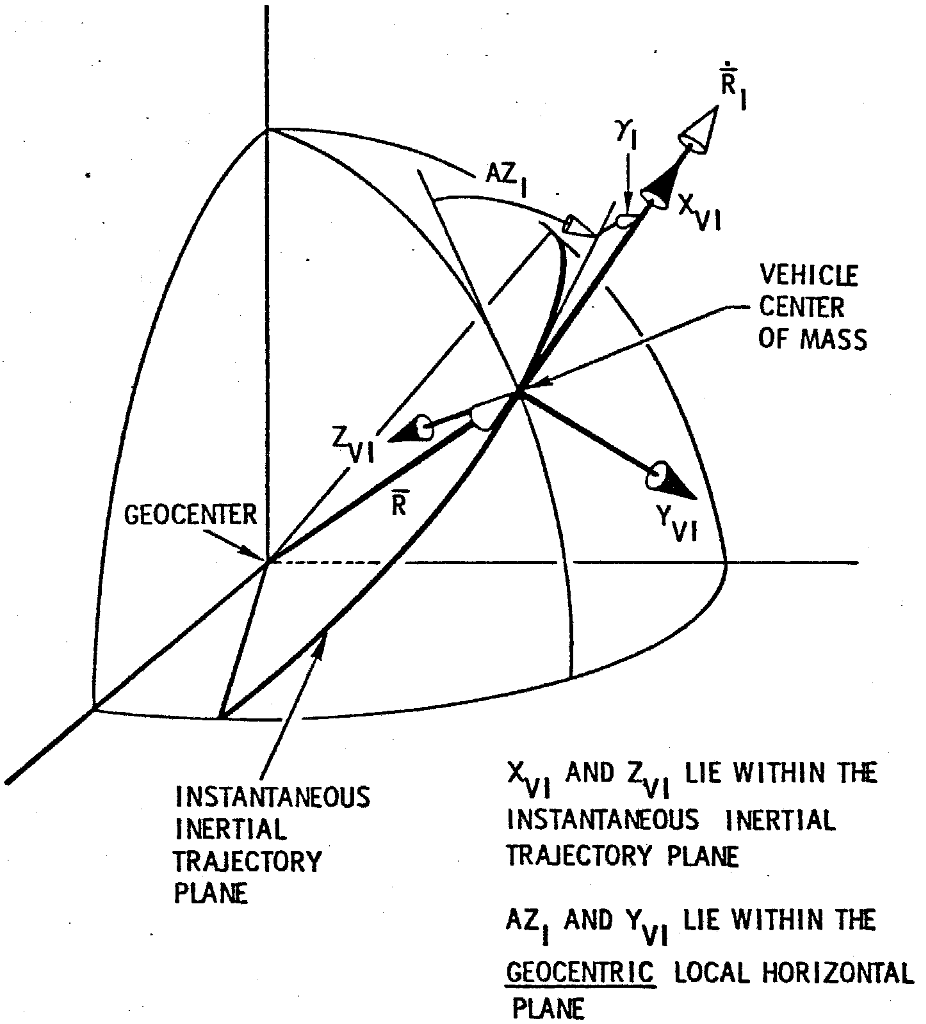

$\bar{R}_I$ VEHICLE POSITION

$\dot{\bar{R}}_I$ INERTIAL VELOCITY

AZ_I INERTIAL AZIMUTH

γ_I INERTIAL FLIGHT PATH ANGLE

2.2 PROBLEM FORMULATION

The equations of motion for the orbit transfer problem can be expressed by the following set of first-order differential equations:

$$\begin{aligned} \dot{\underline{r}} &= \underline{v} \\ \dot{\underline{v}} &= \underline{g}(r) + a\underline{\ell} \\ \dot{m} &= -T/c \end{aligned} \qquad (2.2.1)$$

where

$\underline{r}$ = position vector

$\underline{v}$ = velocity vector

$\underline{g}(\underline{r})$ = acceleration vector due to gravity

a = T/m = acceleration due to the thrust, T

$\underline{\ell}$ = acceleration (or thrust) direction unit vector

m = mass of the spacecraft

c = characteristic exhaust velocity.

A performance index, J, which minimizes the fuel used to perform an orbit transfer is given by

$$J = m(t_o) - m(t_f) \qquad (2.2.2)$$

where t_o is the initial time of the orbit transfer and t_f is the final time of the orbit transfer. The final time t_f is free subject to the condition that a maximum of only three burns is allowed.

A thrust or acceleration limit during the orbit transfer can be represented by either

$$0 \leq T \leq T_{max} \qquad (2.2.3)$$

where T_{max} is the maximum thrust, or

$$0 \leq a \leq a_{max} \tag{2.2.4}$$

where a_{max} is the maximum acceleration.

The boundary conditions at t_o are given by

$$\begin{aligned} \underline{r}(t_o) &= \underline{r}_o \\ \underline{v}(t_o) &= \underline{v}_o \\ m(t_o) &= m_o \end{aligned} \tag{2.2.5}$$

The boundary conditions at t_f can be expressed by the following vector function:

$$\underline{\psi}[\underline{r}(t_f), \underline{v}(t_f)] = \underline{0}; \; (\dim(\underline{\psi}) = q \leq 6) \tag{2.2.6}$$

The problem is to find the optimal time histories of $\underline{\ell}$ and T (i.e., the optimal control history) to minimize the performance index J subject to the constraints given by (2.2.1), (2.2.3) or (2.2.4), (2.2.5), and (2.2.6).

2.3 THE NECESSARY CONDITIONS

2.3.1 The General Problem

Our problem can be formulated as a Mayer problem in the calculus of variations. The analysis will be simplified if we generalize our notation by using state vector control notation. Written in this notation, the problem is to minimize

$$J = \phi[\underline{x}(t_f)] \tag{2.3.1}$$

with respect to u(t), subject to the equations of motion

$$\dot{\underline{x}}(t) = \underline{f}[\underline{x}(t), \underline{u}(t)]; \; \underline{x}(t_o), \, t_o \text{ given; } t_o \leq t \leq t_f, \tag{2.3.2}$$

the inequality constraint

$$\underline{C}[\underline{u}(t),t] \leq \underline{0}, \tag{2.3.3}$$

and the terminal boundary conditions

$$\underline{\psi}[\underline{x}(t_f)] = \underline{0} \tag{2.3.4}$$

where

$\underline{x}(t)$ represents a vector of state variables of dimension n

$\underline{u}(t)$ represents a vector of control variables of dimension m

$\underline{f}$ represents a vector of functions of dimension n

$\underline{C}$ represents a vector of constraint functions of dimension $k \leq m - 1$

$\underline{\psi}$ represents a vector of constraint functions of dimension $q \leq n - 1$

The subscripts 'o' and 'f' indicate evaluation at the initial and final values of the independent variable t, respectively.

The necessary conditions to minimize J are most conveniently expressed in terms of the auxiliary functions

$$H \equiv \underline{\lambda}^T \underline{f} \tag{2.3.5}$$

(known as the Hamiltonian) and

$$\Phi \equiv \phi + \underline{\nu}^T \underline{\psi} \tag{2.3.6}$$

where

$\underline{\lambda}(t)$ represents a vector of continuous Lagrange multipliers (also known as adjoint variables) of dimension n

$\underline{\nu}$ represents a vector of constant Lagrange multipliers of dimension q

The first-order necessary conditions [18] then may be expressed as

$$\dot{\underline{x}} = \underline{f} \tag{2.3.7}$$

$$\underline{x}(t_o),\ t_o \text{ given} \tag{2.3.8}$$

$$\underline{\psi}[\underline{x}(t_f),\ t_f] = \underline{0} \tag{2.3.9}$$

$$\dot{\underline{\lambda}} = -\left(\frac{\partial H}{\partial \underline{x}}\right)^T \tag{2.3.10}$$

$$\left(\frac{\partial H}{\partial \underline{u}} + \underline{\mu}^T \frac{\partial \underline{C}}{\partial \underline{u}}\right)^T = \underline{0} \tag{2.3.11}$$

$$\mu_i(t) \begin{cases} \geq 0, & C_i = 0 \\ = 0 & C_i < 0 \end{cases} \tag{2.3.12a}$$

$$\underline{C}\ [\underline{u}(t),\ t] \leq \underline{0} \tag{2.3.12b}$$

where $\underline{\mu}(t)$ represents a vector of continuous Lagrange multipliers of dimension k and the subscript 'i' denotes an element of a vector;

$$\underline{\lambda}(t_f) = \left(\frac{\partial \Phi}{\partial \underline{x}}\right)^T_{t=t_f} = \left(\frac{\partial \phi}{\partial \underline{x}} + \underline{\nu}^T \frac{\partial \underline{\psi}}{\partial \underline{x}}\right)^T_{t=t_f} \tag{2.3.13}$$

$$H(t_f) = 0 \tag{2.3.14}$$

Equations (2.3.11) and (2.3.12) may be replaced by Pontryagin's "Minimum Principle" which states that H must be minimized over the set of all possible $\underline{u}$. Equations (2.3.13) and (2.3.14) are called the transversality conditions.

Equations (2.3.7) to (2.3.14) constitute a well-posed two-point boundary-value problem (TPBVP). Equation (2.3.11) and the equalities in equation (2.3.12) represent m+k conditions for determining the m component vector $\underline{u}(t)$ and the k component vector $\underline{\mu}(t)$. The solution to the 2n differential equations (2.3.7) and (2.3.10) and the choice of the (q+1) parameters $\underline{\nu}$ and t_f are determined by the (n+q) boundary conditions (2.3.8) and (2.3.9) and the (n+1) transversality conditions (2.3.13) and (2.3.14).

This (n+1) dimensional TPBVP can be put in a more convenient form and reduced to an n dimensional problem by reformulating transversality conditions (2.3.13) and (2.3.14) and by making use of the fact that, in general, t_f can be determined from one component of equation (2.3.9). If we denote this component by $\psi_o[\underline{x}(t_f), t_f]$ and the remaining (q-1) components by $\underline{\hat{\psi}}[\underline{x}(t_f), t_f]$, then (2.3.9) can be written as

$$\psi_o[x(t_f), t_f] = 0 \tag{2.3.15}$$

$$\underline{\hat{\psi}}[\underline{x}(t_f), t_f] = \underline{0} \tag{2.3.16a}$$

Now, equations (2.3.13) and (2.3.14) represent (n+1) equations in the q unknown constant Lagrange multipliers $\underline{\nu}$. Any q of these equations which are linearly independent in the ν's can be solved for these unknown ν's. These values can then be substituted into the remaining equations yielding (n + 1 - q) transversality functions. This reduction can be done either analytically or numerically [16]. The net result is that conditions (2.3.13) and (2.3.14) can be replaced by

$$\underline{T}\,[\underline{x}(t_f),\ \underline{\lambda}(t_f)] = \underline{0} \tag{2.3.16b}$$

where $\underline{T}$ represents an (n + 1 - q) vector of transversality functions. The n dimensional TPBVP then is to determine the n variables $\underline{\lambda}(t_o)$ to satisfy the n boundary conditions (2.3.16).

2.3.2 Thrust-Limited Problem

The necessary conditions to minimize J for the general problem have been given in the previous section. They can be easily specialized to the thrust-limited problem by making the following assignments:

$$\underline{x} = \begin{pmatrix} \underline{r} \\ \underline{v} \\ m \end{pmatrix}, \quad \underline{u} = \begin{pmatrix} \underline{\ell} \\ T \end{pmatrix}, \quad \underline{\lambda} = \begin{pmatrix} \underline{\lambda}_r \\ \underline{\lambda}_v \\ \lambda_m \end{pmatrix}, \quad \phi = m_o - m(t_f)$$
$$\underline{f} = \begin{pmatrix} \underline{v} \\ \underline{g}(\underline{r}) + \frac{T}{m}\underline{\ell} \\ -\frac{T}{c} \end{pmatrix}, \quad C = T(T - T_{max}) \leq 0. \tag{2.3.17}$$

The Hamiltonian is thus

$$H = \underline{\lambda}_r^T \underline{v} + \underline{\lambda}_v^T \underline{g}(\underline{r}) + T/m \, \underline{\lambda}_v^T \underline{\ell} - \lambda_m T/c \tag{2.3.18}$$

The optimality conditions corresponding to (2.3.11) and (2.3.12) can be most easily obtained from the "Minimum Principle". For H to be minimized with respect to $\underline{\ell}$ it follows that

$$\underline{\ell} = -\frac{\underline{\lambda}_v}{\lambda_v} \quad , \quad \lambda_v = |\underline{\lambda}_v| \tag{2.3.19}$$

This result, that $\underline{\ell}$ must be parallel to $\underline{\lambda}_v$, was first found by Lawden [2], who designated $\underline{\lambda}_v$ as the primer vector. Inserting (2.3.19) into (2.3.18) and simplifying yields the following expression for H:

$$H = \underline{\lambda}_r^T \underline{v} + \underline{\lambda}_v^T g(\underline{r}) - \left(\frac{\lambda_v}{m} + \frac{\lambda_m}{c} \right) T \tag{2.3.20}$$

The Hamiltonian is minimized with respect to T, subject to the control inequality constraint (2.2.3), only if

$$T = 0 \quad \text{when} \quad \left(\frac{\lambda_v}{m} + \frac{\lambda_m}{c}\right) < 0$$

$$T = T_{max} \quad \text{when} \quad \left(\frac{\lambda_v}{m} + \frac{\lambda_m}{c}\right) > 0 \qquad (2.3.21)$$

$$0 < T < T_{max} \quad \text{when} \quad \left(\frac{\lambda_v}{m} + \frac{\lambda_m}{c}\right) = 0 \text{ for a finite time}$$

Previous authors have designated

$$K_T = \frac{\lambda_v}{m} + \frac{\lambda_m}{c} \qquad (2.3.22)$$

as the switching function, since its value determines whether the thrust is "on" or "off". $K_T < 0$, $K_T > 0$, and $K_T = 0$ for a finite time correspond to coast arcs, maximum-thrust arcs, and intermediate-thrust arcs respectively. The requirement that $K_T = 0$ for a finite time for intermediate-thrust arcs is made because it is possible that $K_T = 0$ only instantaneously at the "switch times" - the times when T changes instantaneously from 0 to T_{max} or from T_{max} to 0.

The differential equations for $\underline{\lambda}_r$, $\underline{\lambda}_v$, and λ_m are found by taking the negative partial derivatives of H with respect to $\underline{r}$, $\underline{v}$, and m respectively. Thus,

$$\left.\begin{aligned} \dot{\underline{\lambda}}_r &= -\left[\frac{\partial}{\partial \underline{r}}\left(\underline{\lambda}_v^T \underline{g}(\underline{r})\right)\right]^T = -\left(\frac{\partial \underline{g}}{\partial \underline{r}}\right)^T \underline{\lambda}_v \\ \dot{\underline{\lambda}}_v &= -\underline{\lambda}_r \end{aligned}\right\} \qquad (2.3.23)$$

$$\dot{\lambda}_m = -\lambda_v \frac{T}{m^2} \qquad (2.3.24)$$

It is interesting to note that since $\underline{g}(r)$ is obtained by differentiating a potential function with respect to $\underline{r}$, $\frac{\partial \underline{g}}{\partial \underline{r}}$ is a symmetric matrix.

The transversality conditions corresponding to equations (2.3.13) and (2.3.14) are given by

$$\left.\begin{aligned} \underline{\lambda}_r(t_f) &= \left[\left(\frac{\partial \underline{\psi}}{\partial \underline{r}}\right)^T \underline{\nu}\right]_{t=t_f} \\ \underline{\lambda}_v(t_f) &= \left[\left(\frac{\partial \underline{\psi}}{\partial \underline{v}}\right)^T \underline{\nu}\right]_{t=t_f} \end{aligned}\right\} \qquad (2.3.25)$$

$$\lambda_m(t_f) = \left[\frac{\partial(m(t_o) - m(t_f))}{\partial m}\right]_{t=t_f} = -1 \qquad (2.3.26)$$

$$H(t_f) = 0 \qquad (2.3.27)$$

Following the procedure for the general problem in the previous section, the transversality conditions given by (2.3.25) and (2.3.27) can be reduced to a set of (n-q) transversality functions given by

$$\underline{T}\,[\underline{r}(t_f),\ \underline{v}(t_f),\ \underline{\lambda}_r(t_f),\ \underline{\lambda}_v(t_f)] = \underline{0} \qquad (2.3.28)$$

In summary, a set of necessary conditions to minimize J is given by

$$\left.\begin{array}{l}\left.\begin{array}{l}\dot{\underline{r}} = \underline{v} \\ \dot{\underline{v}} = \underline{g}(\underline{r}) + T/m\,\underline{\ell} \\ \dot{m} = -T/c\end{array}\right\}\text{ dimension } 7 \\ \left.\begin{array}{l}\dot{\underline{\lambda}}_r = -\left(\dfrac{\partial \underline{g}}{\partial \underline{r}}\right)^T \underline{\lambda}_v \\ \dot{\underline{\lambda}}_v = -\underline{\lambda}_r \\ \dot{\lambda}_m = -\lambda_v\ T/m^2\end{array}\right\}\text{ dimension } 7\end{array}\right\} \tag{2.3.29}$$

$$\left.\begin{array}{l}\underline{\ell} = -\underline{\lambda}_v/\lambda_v \\ T = 0 \quad \text{when } K_T = \lambda_v/m + \lambda_m/c < 0 \\ T = T_{max} \quad \text{when } K_T = \lambda_v/m + \lambda_m/c > 0 \\ 0 < T < T_{max} \text{ when } K_T = \lambda_v/m + \lambda_m/c = 0 \text{ for finite time}\end{array}\right\} \tag{2.3.30}$$

$$\underline{r}(t_o) = \underline{r}_o\ ,\ \underline{v}(t_o) = \underline{v}_o\ ,\ m(t_o) = m_o\ ,\ t_o \text{ given} \tag{2.3.31}$$

$$\left.\begin{array}{ll}\hat{\underline{\psi}}\,[\underline{r}(t_f),\,\underline{v}(t_f)] = 0 & \text{dimension } (q-1) \le 5 \\ \underline{\mathcal{T}}[\underline{r}(t_f),\underline{v}(t_f),\underline{\lambda}_r(t_f),\underline{\lambda}_v(t_f)]=\underline{0} & \text{dimension } (6-q+1) \\ \lambda_m(t_f) = -1 & \end{array}\right\} \tag{2.3.32}$$

Assuming $K_T \neq 0$ for a finite time, this is a well-posed TPBVP with 7 search variables - $\underline{\lambda}_r(t_o)$, $\underline{\lambda}_v(t_o)$ and $\lambda_m(t_o)$ - to determine so as to satisfy the 7 boundary conditions (2.3.32). (The final time t_f is determined from ψ_o the component of $\underline{\psi}$ not included in $\hat{\underline{\psi}}$.) When $K_T = 0$ for a finite period of time, the problem is singular since T cannot be determined from the given set of equations.

The existence of singular or intermediate-thrust arcs has been investigated by a number of authors, and found to depend on the form of the gravity acceleration vector $\underline{g}(\underline{r})$ and the choice of boundary conditions. The results of these investigations and their bearing on solving practical problems are detailed in Section 2.4.

It is advantageous to note that since H does not depend explicitly on time, $\dot{H} = 0$ on the optimal trajectory. Thus, from (2.3.27), H = 0 on the optimal trajectory, and the number of search variables and boundary conditions can be reduced by one.

2.3.3 The Acceleration - Limited Problem

The necessary conditions for the acceleration-limited problem are very similar to those just obtained for the thrust-limited problem. The differences arise because the acceleration, i.e., T/m, is treated as a control variable instead of T. Rewriting (2.3.20) where we have substituted ma for T yields

$$H = \underline{\lambda}_r^T \underline{v} + \underline{\lambda}_v^T \underline{g}(\underline{r}) - (\lambda_v + \frac{\lambda_m m}{c})a \tag{2.3.33}$$

Thus, H is minimized with respect to a, subject to (2.2.4), only if

$$\left.\begin{array}{lll} a = 0 & \text{when} & (\lambda_v + \frac{\lambda_m m}{c}) < 0 \\ a = a_{max} & \text{when} & (\lambda_v + \frac{\lambda_m m}{c}) > 0 \\ 0 < a < a_{max} & \text{when} & (\lambda_v + \frac{\lambda_m m}{c}) = 0 \text{ for a finite time} \end{array}\right\} \tag{2.3.34}$$

Here we designate the switching function K_a as

$$K_a = \lambda_v + \frac{\lambda_m m}{c} \tag{2.3.35}$$

and note that it is identical to $m\,K_T$, i.e., $K_a = mK_T$.

The differential equations for $\underline{\lambda}_r$ and $\underline{\lambda}_v$ will not change from those found for the thrust-limited problem and are given by (2.3.23). The differential equation for λ_m, however, will be different and is found to be

$$\dot{\lambda}_m = \lambda_m \frac{a}{c} = \lambda_m \frac{T}{mc} \tag{2.3.36}$$

The transversality conditions are the same as those previously given by (2.3.25), (2.3.26) and (2.3.27). Hence the transversality functions (2.3.28) are also valid for this problem.

In summary, a set of necessary conditions to minimize J for the acceleration-limited problem is given by

$$\left.\begin{array}{l} \left.\begin{array}{lll} \dot{\underline{r}} & = & \underline{v} \\ \dot{\underline{v}} & = & \underline{g}(r) + a\,\underline{\ell} \\ \dot{\underline{m}} & = & -\,ma/c \end{array}\right\} \quad \text{dimension 7} \\ \\ \left.\begin{array}{lll} \dot{\underline{\lambda}}_r & = & -\left(\dfrac{\partial \underline{g}}{\partial \underline{r}}\right)^T \underline{\lambda}_v \\ \dot{\underline{\lambda}}_v & = & -\,\underline{\lambda}_r \\ \dot{\lambda}_m & = & \lambda_m\, a/c \end{array}\right\} \quad \text{dimension 7} \end{array}\right\} \tag{2.3.37}$$

$$\left.\begin{aligned} &\underline{\ell} = -\underline{\lambda}_v/\lambda_v \\ &a = 0 \qquad \text{when } K_a = \lambda_v + \frac{\lambda_m m}{c} < 0 \\ &a = a_{max} \qquad \text{when } K_a = \lambda_v + \frac{\lambda_m m}{c} > 0 \\ &0 < a < a_{max} \qquad \text{when } K_a = \lambda_v + \frac{\lambda_m m}{c} = 0 \text{ for a finite time} \end{aligned}\right\} \tag{2.3.38}$$

$$\underline{r}(t_o) = \underline{r}_o,\ \underline{v}(t_o) = \underline{v}_o,\ m(t_o) = m_o,\ t_o \text{ given} \tag{2.3.39}$$

$$\left.\begin{aligned} &\hat{\underline{\psi}}\,[\underline{r}(t_f),\ \underline{v}(t_f)] = \underline{0} \qquad \text{dimension } (q-1) \leq 5 \\ &\underline{T}[\underline{r}(t_f), \underline{v}(t_f), \underline{\lambda}_r(t_f), \underline{\lambda}_v(t_f)] = \underline{0} \qquad \text{dimension } (6-q+1) \\ &\lambda_m(t_f) = -1 \end{aligned}\right\} \tag{2.3.40}$$

As for the thrust-limited problem, this is a well-posed TPBVP except when $K_a = 0$ for a finite period of time. The possibilities of both intermediate thrust and acceleration (i.e., singular) arcs will be treated in the next section.

(An equivalent set of necessary conditions excluding the $\dot{m}$ and $\dot{\lambda}_m$ equations also exists for the acceleration-limited problem. This is possible because, as can easily be verified, $(\dot{\lambda_m m}) = 0$ and thus $\lambda_m m =$ constant. Normalizing the mass such that $m(t_f) = 1$ will allow one to find the optimal control without using the $\dot{m}$ and $\dot{\lambda}_m$ equations. This result could have been directly obtained if the equivalent performance index $\hat{J} = \ln[m(t_o)] - \ln[m(t_f)]$ had been used.)

2.4 THE POSSIBILITY OF SINGULAR ARCS

Rather than treat the thrust and acceleration cases separately, we can, by generalizing our notation, treat both cases together. Let u denote the <u>scalar</u> control variable T or a. From (2.3.20), (2.3.22) and (2.3.33), (2.3.35), we find that

$$\frac{\partial H}{\partial u} = -K_T \text{ for the thrust-limited case,} \tag{2.4.1}$$

$$\frac{\partial H}{\partial u} = -K_a \text{ for the acceleration-limited case.} \tag{2.4.2}$$

We can thus regard $\frac{\partial H}{\partial u}$ as a general switch function with $\frac{\partial H}{\partial u} = 0$ for a finite time as the criterion for a singular arc. Not only is $\frac{\partial H}{\partial u} = 0$ on a singular arc, but so are all the time derivatives of $\frac{\partial H}{\partial u}$. Taking time derivatives of $\frac{\partial H}{\partial u}$ shows that

$$\frac{d^i}{dt^i}\left(\frac{\partial H}{\partial u}\right) = -K_T^{(i)} = -\lambda_v^{(i)}/m = 0 \quad \text{on Intermediate-Thrust arc} \tag{2.4.3}$$

$$\frac{d^i}{dt^i}\left(\frac{\partial H}{\partial u}\right) = -K_a^{(i)} = -\lambda_v^{(i)} = 0 \quad \text{on Intermediate-Acceleration arc} \tag{2.4.4}$$

where $i \geq 1$ denotes the i^{th} time derivative. Thus we see that the existence of singular arcs depends only on the time history of λ_v.

A necessary condition for the optimality of singular arcs known as the generalized Legendre-Clebsch condition (Kelley-Contensou test) is

$$(-1)^p \frac{\partial}{\partial u}\left[\frac{d^{2p}}{dt^{2p}}\left(\frac{\partial H}{\partial u}\right)\right] \geq 0 \tag{2.4.5}$$

for a minimization problem [17]. Since the mass, m, is always positive for a physical problem, we see from (2.4.3) and (2.4.4) that for both the thrust-limited and acceleration-limited problems, this necessary condition can be expressed as

$$(-1)^p \frac{\partial}{\partial u}\left[\lambda_v^{(2p)}\right] \le 0 \qquad (2.4.6)$$

The integer p is the order of the singularity (although Bryson and Ho [18] give this label to 2p) and is determined by taking successive time derivatives of $\frac{\partial H}{\partial u}$, or equivalently λ_v, until the control u appears. Not only does this differentiation procedure give twice the order of the singularity, but it also allows us to find an expression for u on the singular arc. Four successive differentiations of λ_v and use of either (2.3.29) and (2.4.3) or (2.3.37) and (2.4.4) yield [21]

$$0 = \underline{\lambda}_v^T \underline{\lambda}_r \qquad (2.4.7)$$

$$0 = \underline{\lambda}_v^T \left(\frac{\partial \underline{g}}{\partial \underline{r}}\right)^T \underline{\lambda}_v + \underline{\lambda}_r^T \underline{\lambda}_r \qquad (2.4.8)$$

$$0 = \frac{\partial}{\partial \underline{r}}\left[\underline{\lambda}_v^T \left(\frac{\partial \underline{g}}{\partial \underline{r}}\right)^T \underline{\lambda}_v\right]\underline{v} - 4\underline{\lambda}_v^T \left(\frac{\partial \underline{g}}{\partial \underline{r}}\right)^T \underline{\lambda}_r \qquad (2.4.9)$$

$$0 = -\frac{T}{m}\, q(\underline{r}, \underline{v}, \underline{\lambda}_r, \underline{\lambda}_v) + W(\underline{r}, \underline{v}, \underline{\lambda}_r, \underline{\lambda}_v) \qquad (2.4.10)$$

Thus, for both the thrust-limited and acceleration-limited problem, $\bar{p}=2$ and the thrust on a singular arc is given by

$$T = m \frac{W(\underline{r},\underline{v},\underline{\lambda}_r,\underline{\lambda}_v)}{q(\underline{r},\underline{v},\underline{\lambda}_r,\underline{\lambda}_v)} \tag{2.4.11}$$

Also, for both problems, we find by inserting (2.4.10) into (2.4.6) that the necessary condition for optimality of the singular arc becomes

$$q(\underline{r},\underline{v},\underline{\lambda}_r,\underline{\lambda}_v) \geq 0 \tag{2.4.12}$$

Because T is non-negative and bounded, (2.4.11) implies that if W and q are not simultaneously zero, then (2.4.12) can be strengthened to

$$q(\underline{r},\underline{v},\underline{\lambda}_r,\underline{\lambda}_v) > 0 \tag{2.4.13}$$

and in addition

$$W(\underline{r},\underline{v},\underline{\lambda}_r,\underline{\lambda}_v) > 0 \tag{2.4.14}$$

on a singular arc.

The question as to whether optimal singular arcs exist for the orbit transfer problem has been investigated by a number of authors [2, 17-29] over the past 20 years. This investigation has been concentrated in two distinct areas - the existence and characterization of regions in $\underline{r}$ - $\underline{v}$ space where the above necessary conditions are satisfied and the existence and characterization of necessary conditions at the junctions joining nonsingular and singular arcs.

With regard to the first area, Lawden [2] first proposed a singular arc for the free terminal time case where the gravity acceleration magnitude, $g(r)$, is of the form $1/r^2$ (i.e., a "spherical earth" gravity). The singular arc trajectory takes the form of a spiral <u>coplanar</u> transfer and has become known as Lawden's spiral. Robbins [21] and others, [22], have since proved that Lawden's spiral is not optimal. Archenti and Vinh [23] later showed that in the equatorial plane of an "oblate earth" where $g(r) = f(1/r^2, 1/r^4)$, Lawden's spiral <u>may</u> be optimal. But Teschner [25] then showed that this was true only if a circular coasting arc did not form any part of the optimal trajectory. Teschner expanded this result to include any coplanar transfer in which $g(r)/r$ is a monotonic decreasing function with r. To date, the author is unaware of any investigation into the optimality of <u>three</u>-dimensional singular arcs.

Robbins [21] first considered the junction conditions for the orbit transfer problem and felt it probable that only for certain special boundary conditions would a singular arc exist, with the consequence that the thrust on the nonsingular arc would alternate between zero and its maximum value at an infinite frequency. McDanell and Powers [27] provided additional insight into junction conditions by clarifying and extending the necessary conditions concerning the continuity and smoothness of a <u>piecewise analytic</u>

optimal control at a junction. New necessary conditions were also provided to aid in characterizing problems which might possess nonanalytic junctions. McDanell and Powers stated that their conditions assuming piecewise analytic control would probably not apply to singular arcs of even order since their experience indicated that junctions for these singular arcs were nonanalytic. Breakwell and Dixon [28] made a notable contribution by completely characterizing the junction conditions for the orbit transfer problem. Through consideration of the secondary accessory minimum problem (i.e., minimization of the second variation of the performance index) they showed that the singular surface is a four-dimensional manifold in a six-dimensional state space obtained through a coordinate transformation on $\underline{r}$ and $\underline{v}$. To maintain continuity of the state variables for general boundary conditions, a short period of strong variations in the acceleration (or thrust) is required. The nature of these strong variations - found by minimizing the change in the performance index up to (but not including) third order terms - is characterized by an infinite number of switches between maximum and zero thrust during the short period. Thus, the suspicions of Robbins were verified. Bershchanskii [29] later generalized this result for any optimal control problem having an even order of singular control where the control is a bounded scalar. These junction conditions are physically unrealizable and thus have only a theoretical significance.

A review of the published work therefore shows that an optimal three-dimensional singular arc for the orbit transfer problem may exist, but that it is physically impossible to join this arc to a nonsingular arc. Thus, the possibility of a singular arc occurring for a practical problem need not be considered if nonsingular arcs are allowed.

Chapter 3

SOLUTION OF THE OPTIMAL CONTROL PROBLEM

3.1 CHOICE OF METHOD

Rewriting equations (2.3.1) - (2.3.4), our problem is to minimize

$$J = \phi[\underline{x}(t_f)] \tag{3.1.1}$$

with respect to $\underline{u}(t)$, subject to the equations of motion

$$\dot{\underline{x}}(t) = \underline{f}[\underline{x}(t),\ \underline{u}(t)];\ \underline{x}(t_o),\ t_o \text{ given};\ t_o \leq t \leq t_f, \tag{3.1.2}$$

the inequality constraint

$$\underline{C}[\underline{u}(t),t] \leq \underline{0}, \tag{3.1.3}$$

and the terminal boundary conditions

$$\underline{\psi}\,[\underline{x}(t_f)] = \begin{pmatrix} \psi_o[\underline{x}(t_f)] \\ \hdashline \hat{\psi}\,[\underline{x}(t_f)] \end{pmatrix} = \underline{0} \tag{3.1.4}$$

As was seen in Section 2.3, through use of the first-order necessary conditions, this problem can be posed as a nonlinear TPBVP:

$$\dot{\underline{x}} = \underline{f}(\underline{x},\underline{u}),\ t_o \leq t \leq t_f \tag{3.1.5}$$

$$\underline{\dot{\lambda}} = -\left[\frac{\partial H}{\partial \underline{x}}(\underline{x},\underline{\bar{u}},\underline{\lambda})\right]^T, \; t_o \le t \le t_f \tag{3.1.6}$$

$$\underline{x}(t_o), \; t_o \text{ given} \tag{3.1.7}$$

$$\underline{\hat{\psi}}[\underline{x}(t_f)] = \underline{0} \tag{3.1.8}$$

$$\underline{T}[\underline{x}(t_f), \underline{\lambda}(t_f)] = \underline{0} \tag{3.1.9}$$

$$t_f \text{ determined from } \psi_o[\underline{x}(t_f)] = 0 \tag{3.1.10}$$

where

$$H \equiv \underline{\lambda}^T \; \underline{f}\,(\underline{x},\underline{u}) \tag{3.1.11}$$

$$\underline{\bar{u}} = \arg \min_{\underline{u}}(H) \text{ subject to } \underline{C}(\underline{u},t) \le \underline{0} \tag{3.1.12}$$

Blank and Shinar [30] have performed a recent study and comparison of four basic methods to solve this type of problem. These four methods consisted of a direct method - the sequential gradient projection-restoration algorithm (SGPRA) - and three indirect methods - the modified quasilinearization algorithm (QUASIM), the Neighboring Extremals Algorithm (NEEXT), and the Direct Shooting Algorithm (DSA).

Blank and Shinar tabulated the main characteristics of the algorithms as follows:

Table 3.1 Comparison of Algorithms

Method	Implementation	Formulation	Computer Storage	Convergence Sensitivity	Convergence Speed
SGPRA	complex	simple	high	very good	Initial: high Terminal: low
QUASIM	simple	complex	high	poor	high
NEEXT	simple	complex	low	poor	high
DSA	very simple	very simple	low	good	Initial: low Terminal: high

Convergence sensitivity, or robustness, (i.e. the capability of the algorithm to converge for poor initial guesses) and convergence speed are measures of the computational efficiency of the optimization algorithm. For problems with noncontinuous control, such as thrust switches, Blank and Shinar advocate using a combination algorithm of SGPRA and DSA. (The second-order methods QUASIM and NEEXT cannot be used directly if the control is discontinuous.) This combination would result in very good computational efficiency, but at the expense of implementation, formulation, and computer storage.

A better approach, if it can be found, might be to modify the DSA method in such a way as to preserve the good characteristics and improve the convergence sensitivity and the initial convergence speed.

A candidate approach presented by Hersom, Dixon, Bartholomew-Biggs, and Pocha [11] for solving orbit transfer problems converts the indirect DSA method into a hybrid (i.e. combination of indirect and direct) nonlinear programming (HNLP) method which is even simpler to implement and formulate. The HNLP method should be more robust than the DSA method since it minimizes the performance index directly as will be seen below.

Hersom, et al, include another modification first presented by Dixon and Biggs [31], called an Adjoint-Control Transformation (ACT), which has been found to increase both robustness and convergence speed when applied to the DSA method. The ACT will be discussed in Section 3.3.

Incorporating both modifications results in a method (which will be referred to as the HNLP/ACT method) which eliminates the faults and improves the advantages of the DSA method. The HNLP method, in fact, offers a solution technique for many quite general optimal control problems with a minimum of effort, by taking advantage of the excellent NLP algorithms developed over the years.

The next section presents an analysis of the HNLP method for a class of general optimal control problems.

3.2 THE HYBRID NONLINEAR PROGRAMMING (HNLP) METHOD

The DSA method for solving the TPBVP given by equations (3.1.5) - (3.1.12) is an iterative technique for improving estimates of $\underline{\lambda}(t_o)$ (the search or optimization variables) so as to satisfy the specified terminal conditions, equations (3.1.8) and (3.1.9). Two basic approaches exist for implementing this technique. The first approach considers $\underline{\hat{\psi}}$ and $\underline{T}$ as implicit functions of $\underline{\lambda}(t_o)$ and finds the simultaneous solution of the set of nonlinear equations $\underline{\hat{\psi}} = \underline{0}$ and $\underline{T} = \underline{0}$ by some modification of Newton's method. This approach can be posed as:

$$\left.\begin{array}{ll} \text{Find} & \underline{\lambda}(t_o) \\ \text{such that} & \underline{\hat{\psi}}[\underline{\lambda}(t_o)] = \underline{0} \\ & \underline{T}[\underline{\lambda}(t_o)] = \underline{0} \end{array}\right\} \qquad (3.2.1)$$

The second approach [32] considers the cumulative error in the terminal conditions as an implicit function of $\underline{\lambda}(t_o)$ and finds the minimum of this error function through use of an NLP algorithm. At the minimum of the error function $\underline{\hat{\psi}} = \underline{0}$ and $\underline{T} = \underline{0}$. If the error function is of the form

$$E[\underline{\lambda}(t_o)] = \underline{\hat{\psi}}^T\underline{\hat{\psi}}[\underline{\lambda}(t_o)] + \underline{T}^T\underline{T}\ [\underline{\lambda}(t_o)],$$

then this second approach can be posed as the following NLP problem:

$$\min_{\underline{\lambda}(t_o)} \left| \underline{\hat{\psi}}^T \underline{\hat{\psi}}\ [\underline{\lambda}(t_o)] + \underline{T}^T\underline{T}\ [\underline{\lambda}(t_o)] \right| \qquad (3.2.2)$$

Various combinations of these two approaches can also be used to formulate the problem. One such formulation might be to pose it as:

$$\left.\begin{array}{ll} & \min\limits_{\underline{\lambda}(t_o)} \ \underline{T}^T\underline{T}\ [\underline{\lambda}(t_o)] \\ \text{such that} & \underline{\hat{\psi}}[\underline{\lambda}(t_o)] = \underline{0} \end{array}\right\} \qquad (3.2.3)$$

It is this formulation which suggests the HNLP method.

The HNLP method is very similar to the DSA formulation of (3.2.3) but differs in one important respect. Instead of minimizing the cumulative error in the transversality functions, the HNLP method directly minimizes the performance index, equation (3.1.1). In other words, the HNLP method considers ϕ and $\underline{\hat{\psi}}$ as implicit functions of $\underline{\lambda}(t_o)$ and poses the NLP problem as:

$$\left.\begin{aligned} &\min_{\underline{\lambda}(t_o)} \ \phi[\underline{\lambda}(t_o)] \\ &\text{such that } \underline{\hat{\psi}}[\underline{\lambda}(t_o)] = \underline{0} \end{aligned}\right\} \qquad (3.2.4)$$

By posing the problem this way, the transversality functions are implicitly satisfied by the NLP algorithm at the solution; hence, they do not even have to be derived. Thus, if the HNLP method is used to solve the optimal control problem given by (3.1.1) - (3.1.4), then the only additional equations which need be derived are (3.1.6), (3.1.11) and (3.1.12).

Besides being easier to implement and formulate, the HNLP method has one other advantage over the DSA method. Because the performance index, rather than an error function obtained from the first order variation of the performance index, is being minimized directly, a larger convergence domain should exist. That is, the method should be more robust.

The next section details a transformation of the optimization variables which has been shown to also increase robustness.

3.3 THE ADJOINT - CONTROL TRANSFORMATION ACT

As we have seen, the solution to an optimal control problem by the HNLP (or DSA) method involves finding the values of the initial adjoint variables, $\underline{\lambda}(t_o)$, which satisfy the first order necessary conditions. We will call these variables the optimization variables and denote their optimum value by $\underline{\lambda}^*(t_o)$. The function of the NLP algorithm then, is to find $\underline{\lambda}^*(t_o)$ beginning from some initial guess for the optimization variables which we will denote by $\underline{\lambda}^o(t_o)$.

Unfortunately, systems of state and adjoint equations have the characteristic that terminal conditions are often very sensitive to changes in $\underline{\lambda}(t_o)$. Thus, a poor choice for $\underline{\lambda}^o(t_o)$ could result in very large terminal condition errors. This accounts for the low initial convergence speed and lackluster convergence sensitivity of the DSA method. Dixon et al [31] have found, however, that both of these performance criteria can be improved through use of an Adjoint-Control Transformation (ACT), which results in initial values of control variables and their derivatives being used as the optimization variables instead of $\underline{\lambda}(t_o)$.

The use of control related variables rather than $\underline{\lambda}(t_o)$ as the optimization variables is also desirable from the standpoint of good initial guesses. Mathematically, $\underline{\lambda}(t_o)$ is the influence vector on J, the optimal performance index, of changes in the initial conditions of the state variables, i.e.

$$\underline{\lambda}(t_o) = \left(\frac{\partial J}{\partial \underline{x}(t_o)}\right)^T .$$

While this may offer some physical insight into the nature of $\underline{\lambda}(t_o)$, it is not very useful for providing good initial guesses. Control-related variables, on the other hand, typically have much greater physical significance. Their optimal values can usually be reasonably well estimated based on the physical insights gained from the solutions of related problems.

The ACT for the thrust-limited problem will be derived using equations (2.3.29) - (2.3.32). The results obtained will also apply for the acceleration-limited problem.

We first observe that at a switch point, i.e., when $t=t_s$, the switching function K_T is zero. Thus

$$\lambda_v(t_s) = -\left.\frac{m\lambda_m}{c}\right|_{t_s} \tag{3.3.1}$$

Also, we observe that $\underline{\lambda}_v$ can be expressed as the following function of $\underline{\ell}$:

$$\underline{\lambda}_v = -\lambda_v \underline{\ell}. \tag{3.3.2}$$

Hence, if $\underline{\ell}(t_s)$ is known, $\underline{\lambda}_v(t_s)$ can be found from (3.3.2), i.e.,

$$\underline{\lambda}_v(t_s) = -\lambda_v(t_s)\,\underline{\ell}(t_s). \tag{3.3.3}$$

We next attempt to find $\underline{\lambda}_r(t_s)$ in terms of control related variables. From (2.2.27) we see that

$$\underline{\lambda}_r = -\dot{\underline{\lambda}}_v \tag{3.3.4}$$

Differentiating (3.3.2) and combining the result with the above equation yields

$$\underline{\lambda}_r = \dot{\lambda}_v \underline{\ell} + \lambda_v \dot{\underline{\ell}} \qquad (3.3.5)$$

We would have our desired result if $\dot{\lambda}_v(t_s)$ were known. Since the Hamiltonian H is zero on the optimal trajectory, we know that at a switch point

$$\left.(\underline{\lambda}_r^T \underline{v} + \underline{\lambda}_v^T \underline{g})\right|_{t_s} = 0. \qquad (3.3.6)$$

Substituting for $\underline{\lambda}_r$ from (3.3.5) and $\underline{\lambda}_v$ from (3.3.2) and rearranging gives

$$\dot{\lambda}_v(t_s) = -\lambda_v(t_s) \left.\frac{\dot{\underline{\ell}}^T \underline{v} - \underline{\ell}^T \underline{g}}{\underline{\ell}^T \underline{v}}\right|_{t_s} \qquad (3.3.7)$$

Thus, from (3.3.5)

$$\underline{\lambda}_r(t_s) = -\lambda_v(t_s) \left.\left[\frac{\dot{\underline{\ell}}^T \underline{v} - \underline{\ell}^T \underline{g}}{\underline{\ell}^T \underline{v}} \underline{\ell} - \dot{\underline{\ell}}\right]\right|_{t_s} \qquad (3.3.8)$$

The ACT, therefore, consists of (3.3.1), (3.3.3), and (3.3.8). These equations apply for both the thrust-limited and acceleration-limited problems. Assuming $\lambda_v(t_s)$ can be computed, $\underline{\lambda}_r(t_s)$ and $\underline{\lambda}_v(t_s)$ can be found from $\underline{\ell}(t_s)$ and $\dot{\underline{\ell}}(t_s)$ - the thrust pointing vector and the derivative of the thrust pointing vector. Since $\underline{\ell}$ is a unit vector it is possible to express both $\underline{\ell}$ and $\dot{\underline{\ell}}$ as functions of two pointing angles and their derivatives, i.e. $\underline{\ell} = \underline{\ell}(\alpha, \beta)$ and $\dot{\underline{\ell}} = \dot{\underline{\ell}}(\alpha, \beta, \dot{\alpha}, \dot{\beta})$.

The computation of $\lambda_v(t_s)$ deserves further consideration. Since $m(t_o)$ is given, $m(t_s)$ can be obtained by numerically integrating the $\dot{m}$ equation forward. This cannot be done, however, for $\lambda_m(t_s)$ since $\lambda_m(t_o)$ is not known. We do know, though, that $\lambda_m(t_f) = -1$. Also since $\dot{\lambda}_m \leq 0$, we know that λ_m like m, is a monotonically decreasing function. If t_{s_1} denotes the time when the switch function first becomes positive (i.e., the ignition time of the first burn), then $t_o \leq t_{s_1}$. Since $\dot{m}$ and $\dot{\lambda}_m$ are zero when the thrust is zero,

$$\lambda_m(t_o) = \lambda_m(t_{s_1}) = -\lambda_v(t_{s_1})\, c/m_o.$$

Since $\lambda_v = |\underline{\lambda}_v|$ and must be nonzero at t_{s_1} for the control to be defined, we can deduce that $\lambda_m(t_o) < 0$ and therefore $0 > \lambda_m(t) \geq -1$ for $t_o \leq t \leq t_f$. An analysis of the adjoint equations in either (2.3.29) or (2.3.37) reveals that they can be normalized by $|\lambda_m(t_o)|$ without affecting the computation of the control. We will therefore have an equally valid set of first order necessary conditions by specifying that $\lambda_m(t_o) = -1$ instead of $\lambda_m(t_f) = -1$. Thus $\lambda_m(t_s)$ can be obtained, like $m(t_s)$, by numerically integrating forward the $\dot{\lambda}_m$ equation from $\lambda_m(t_o) = -1$, and so $\lambda_v(t_s)$ can be computed for a given t_s. Since t_{s_1} is not usually known apriori, it would have to be included with the optimization variables.

3.4 HNLP/ACT PROBLEM FORMULATION

The HNLP/ACT method for the solution of the thrust-limited or acceleration-limited optimal control orbit transfer problem can be formulated as follows:

$$\left.\begin{aligned}
&\underset{\underline{z}}{\text{Min}} \quad [m(t_o) - m(t_f)] \\
&\text{such that} \quad \underline{\hat{\psi}}[\underline{r}(t_f), \underline{v}(t_f)] = \underline{0} \\
&\text{where the vector } \underline{z} \text{ of optimization variables is given by} \\
&\underline{z} = \begin{pmatrix} \alpha(t_{s_1}) \\ \beta(t_{s_1}) \\ \dot{\alpha}(t_{s_1}) \\ \dot{\beta}(t_{s_1}) \\ t_{s_1} \end{pmatrix}
\end{aligned}\right\} \qquad (3.4.1)$$

and where $\underline{\hat{\psi}}$ and $[m(t_o) - m(t_f)]$ are related to the optimization variables through

$$\left.\begin{aligned}
\underline{\dot{r}} &= \underline{v} \\
\underline{\dot{v}} &= \underline{g}(r) + T/m\ \underline{\ell} \\
\dot{m} &= -T/c \\
\underline{\dot{\lambda}}_r &= -\left(\frac{\partial \underline{g}}{\partial \underline{r}}\right)^T \underline{\lambda}_v \\
\underline{\dot{\lambda}}_v &= -\underline{\lambda}_r \\
\dot{\lambda}_m &= \begin{cases} -\lambda_v\ T/m^2 & \text{for thrust-limited case} \\ \lambda_m\ T/mc & \text{for acceleration-limited case} \end{cases}
\end{aligned}\right\} \quad t_{s_1} \le t \le t_f$$

$$T \begin{cases} = 0 & \text{when } \lambda_v + \dfrac{\lambda_m m}{c} < 0 \\ = T_{max} & \text{when } \lambda_v + \dfrac{\lambda_m m}{c} > 0 \end{cases} \quad \text{for thrust-limited case}$$

$$T \begin{cases} = 0 & \text{when } \lambda_v + \dfrac{\lambda_m m}{c} < 0 \\ = m a_{max} & \text{when } \lambda_v + \dfrac{\lambda_m m}{c} > 0 \end{cases} \quad \text{for acceleration-limited case}$$

with $\underline{r}(t_{s_1})$, $\underline{v}(t_{s_1})$, $m(t_{s_1})$, $\lambda_m(t_{s_1})$ computed from

$$\left.\begin{aligned} \dot{\underline{r}} &= \underline{v} \quad , \underline{r}(t_o) = \underline{r}_o \\ \dot{\underline{v}} &= \underline{g}(r) \; , \underline{v}(t_o) = \underline{v}_o \\ \dot{m} &= 0 \quad , m(t_o) = m_o \\ \dot{\lambda}_m &= 0 \quad , \lambda_m(t_o) = -1 \end{aligned}\right\} t_o \leq t \leq t_{s_1}$$

and $\underline{\lambda}_r(t_{s_1})$, $\underline{\lambda}_v(t_{s_1})$ computed from

$$\underline{\ell}(t_{s_1}) = \underline{\ell}\left[\alpha(t_{s_1}), \beta(t_{s_1})\right]$$

$$\dot{\underline{\ell}}(t_{s_1}) = \dot{\underline{\ell}}\left[\alpha(t_{s_1}), \beta(t_{s_1}), \dot{\alpha}(t_{s_1}), \dot{\beta}(t_{s_1})\right]$$

$$\lambda_v(t_{s_1}) = -\frac{m(t_{s_1})\ \lambda_m(t_{s_1})}{c}$$

$$\underline{\lambda}_r(t_{s_1}) = -\lambda_v(t_{s_1}) \left[\frac{\dot{\underline{\ell}}^T \underline{v} - \underline{\ell}^T \underline{g}}{\underline{\ell}^T \underline{v}} \quad \underline{\ell} - \dot{\underline{\ell}} \right] \Bigg|_{t_{s_1}}$$

$$\underline{\lambda}_v(t_{s_1}) = -\lambda_v(t_{s_1})\ \underline{\ell}(t_{s_1})$$

Instead of using the switching function to determine the number of burns, it is much more convenient to specify the number of burns a priori. This is easily done by including the ignition and burnout times for the burns as optimization variables. In addition, one could also use the ACT to reinitialize the adjoint equations at the beginning of each burn. This may prove helpful if some insightful information is known about the pointing of the thrust vector during the burns.

Although not required, additional constraints may also be included in the formulation to help "guide" the optimization process toward the optimal solution. Examples of such constraints are requirements that the switching function be zero at the beginning and end of each burn.

These decisions must be based on the accuracy of initial guesses and the characteristics of the NLP algorithm. One of the advantages of the HNLP method is that various combinations of optimization variables and constraints can be tried until a proper "mix" of robustness and convergence speed are obtained.

Chapter 4

NUMERICAL RESULTS FOR SEVERAL CLASSES OF ORBIT TRANSFERS

4.1 SPECIFICATION OF PROGRAM PARAMETERS AND TECHNIQUES

4.1.1 Earth and Spacecraft Constants

A spherical, non-rotating earth model was used for this study. Thus the gravity vector referred to in equation (2.2.1) is given by

$$\underline{g}(r) = -\frac{\mu}{r^3}\underline{r} \quad (4.1.1)$$

where μ is the earth gravitational constant. The values used for earth radius, r_e, and μ were

r_e = 20925721.78 feet (6378160 meters)

μ = $1.407653916 \times 10^{16}$ ft^3/sec^2

To facilitate comparisons with earlier studies, the specific impulse of the spacecraft was chosen to be 450 secs.

4.1.2 Integrator and Propagator

During periods of nonzero thrust, the equations of motion were numerically integrated using an Adams-Moulton, variable step, eighth order integration scheme. The scheme chooses the step size to maintain the estimated error below a given upper bound. The estimated error is computed in such a way that for magnitudes of the integration variables greater or less than one, the error is, respectively, a relative or absolute measure of the accuracy. The upper bound used for this study was 10^{-9}.

During coast phases (i.e., periods of zero thrust) the system of equations given by (2.3.29) for the thrust-limited case and (2.3.37) for the acceleration-limited case are identical. Inspection of these equations reveals that m and λ_m remain constant during a coast. Use of (4.1.1) for the gravity vector allows the remaining equations to be analytically integrated. The details of this procedure have been given by Vinh [33]. The independent variable used to propagate $\underline{r}$, $\underline{v}$, $\underline{\lambda}_r$, and $\underline{\lambda}_v$ was chosen to be the coast angle. The corresponding coast time is easily computed using Kepler's equation.

The use of a propagator during the coast phases resulted in a significant savings in computation costs, since the coast arcs were usually quite large.

4.1.3 The NLP Algorithm

The NLP algorithm used in this study was developed by J.T. Betts and is described in detail in Reference 34. The general features of the algorithm allow it to solve problems containing both equality and inequality constraints. Betts uses an approach which does not require explicit evaluation of gradient information. Thus implementation and formulation of an NLP problem is straightforward and simple. A central feature of the method is the use of an orthogonal decomposition of the problem variables into "optimization" and "constraint elimination" variables. The constraint elimination is accomplished using a generalized secant method in the transformed variables. A finite difference Newton method is used to perform the unconstrained minimization process. The overall solution to the NLP problem requires solving a sequence of equality constrained problems defined by an active set strategy.

Numerical experience with the algorithm indicates that it is among the best of the available methods for solving the general NLP problem. Thus, selection of this algorithm is an appropriate choice for use in solving the problems described in this chapter.

4.1.4 Choice of Variables and Constraints

4.1.4.1 Choice of Variables

The selection of variables and constraints was predicated, to a large degree, on the behavior of the switching function K (i.e., K_T for the thrust-limited problem and K_a for the acceleration-limited problem). For a typical optimal finite 3-burn orbit transfer, the switching function behaves as illustrated in Figure 6. In general it was found, however, that the behavior of the switching function was very sensitive to the initial values of the adjoint variables. It was not unusual for a given initial guess to cause K to remain completely positive or negative during several revolutions of the spacecraft about the earth. This sensitivity makes K a very undesirable parameter for determining when to thrust or coast. A much more

Figure 6. Optimal Form of Switching Function

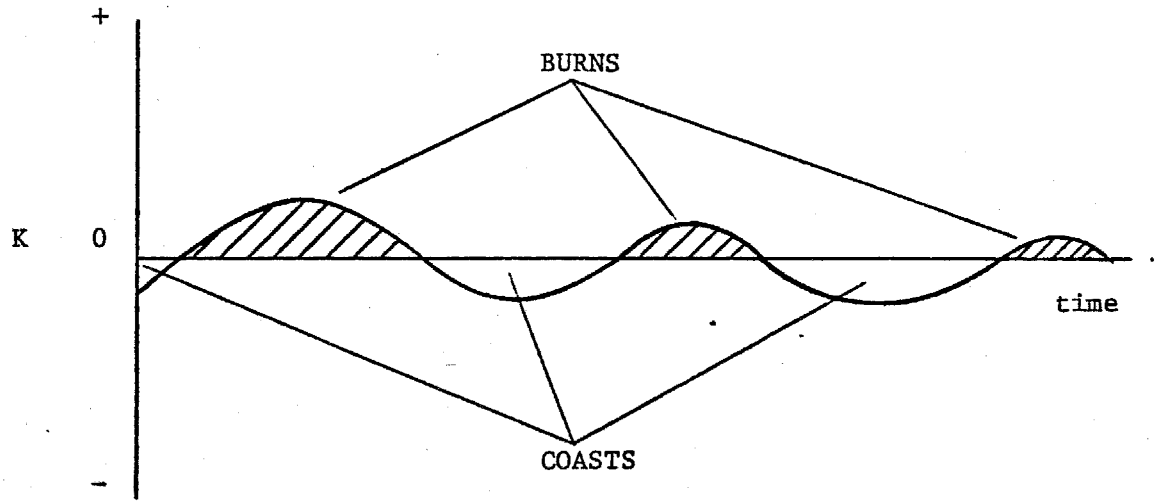

robust technique is to introduce burn times and coast times (or angles) as additional variables in the problem. The optimization algorithm will choose these variables so that at the solution the switching function will be positive during the burns and negative during the coasts. A word of caution must be made about this technique, however. The optimization procedure is capable of removing nonoptimal burns or coasts, but is not able to "add in" optimal ones. Thus, the problem must be formulated with the maximum number of burns which will insure an optimal solution. Due to the nature of the present study, this requirement resulted in two additional coast times and three burn times being included among the vector $\underline{z}$ of optimization variables given in (3.4.1).

Included among the optimization variables of (3.4.1) are the pointing angles α and β and their time derivatives $\dot{\alpha}$ and $\dot{\beta}$. These angles are the pitch and yaw angles, respectively, of an Euler yaw, pitch, roll sequence from a given reference frame to the spacecraft body frame. The spacecraft body frame is a righthanded coordinate frame with the positive x-axis directed along the thrust vector. It should be noted that since we are only interested in the orientation of the thrust vector with respect to the reference frame, the roll angle may be ignored. Any of the three coordinate frames depicted in Figures 1, 4 and 5 are appropriate reference frames. Hereafter, the reference frame used will be denoted by using a mnemonic for the frame as a subscript.

As mentioned earlier, the optimization variables include coast times. Coast angles, however, could just as easily be used. In fact, since the use of coast angles rather than coast times makes it easier to visualize the movement of a spacecraft during a coast, the coast angles rather than the times were the preferred optimization variables.

Prior to solving an optimal finite burn orbit transfer problem, the geometrically similar impulsive burn orbit transfer problem was solved using the NLP algorithm. The optimization variables for this problem consisted of the impulsive velocity increments and pointing angles for each burn and the coast angles. Once the solution was obtained, this impulsive (i.e., infinite initial thrust to weight ratio) burn solution served as the initial guess for the high thrust (i.e., initial thrust to weight ratio of one) finite burn problem. Rather than using the impulsive burn solution to only initialize the adjoint equations (through the ACT) at the beginning of the trajectory, it was found to be much more advantageous to reinitialize the adjoint equations at the beginning of every burn. Although this involved using more optimization variables, greater control was maintained over the type of initial trajectory which was flown. After the optimization had progressed for awhile, this reinitialization procedure was discontinued.

4.1.4.2 Choice of Constraints

Besides the set of terminal constraints given by $\hat{\underline{\psi}}[\underline{r}(t_f, \underline{v}(t_f)] = \underline{0}$, additional constraints, although not required, were included in the problem formulation to help "guide" the optimization process toward the optimal solution. These additional constraints consisted of requirements that the switching function be zero at the beginning and end of each burn. Inclusion of these "switching constraints" resulted in a dramatic improvement in the convergence speed of the optimization algorithm. An analysis of the behavior of the Hamiltonian during the optimization process offers a possible explanation for this improvement.

Using equations (2.3.29) through (2.3.32), it is not difficult to show that the time derivative of the Hamiltonian, $\dot{H}$, is given by

$$\dot{H} = K_T \dot{T} \tag{4.1.2}$$

where $\dot{T}$ may include delta functions. Thus $H(t_f)$ is given by

$$H(t_f) = H(t_o) + \sum_{i=1}^{j} K_T(t_i)\ \Delta T(t_i) \tag{4.1.3}$$

where t_i denotes a switch point and j is the total number of switch points. The value of ΔT will be either T_{max} or $-T_{max}$ depending on whether the switch point is between a coast and a burn or a burn and a coast. We thus see that on a nonoptimal trajectory, H is given by a step function with the sizes and directions of the "steps" determined by the values of ΔT and K_T at the switch points. An optimal trajectory would of course have all the $K_T(t_i)$ zero. It should also be noted that since H=0 on the optimal trajectory, we can set $H(t_o) = 0$. The requirement that H=0 on the trajectory can thus be formulated as the following problem:

Find t_i

such that $K_T(t_i) = 0$

Hence, the inclusion of the switching constraints in the problem which uses burn times and coast times (or angles) as optimization variables is equivalent to requiring that H=0 on the optimal trajectory. The explicit statement of this constraint, which is actually a transversality condition and a set of corner conditions, helps the NLP algorithm find the optimal solution more quickly probably because the number of implicit transversality functions which must now be satisfied is decreased by (1+j).

4.2 COMPARISON WITH RESULTS OF REDDING

A comparison with some of the published results of Redding [13] was made to validate the optimization procedure. Redding found solutions for optimal finite burn transfers from a 28.5 degree inclined, 119.78 nmi altitude (corresponding to a 6600 km radius) circular orbit to Geosynchronous orbit. Although Redding did not present the transfer orbits or the total velocity increments required, he did present the differences in the total velocity increments between the impulsive burn transfer and various finite burn transfers.

Table 2 compares the results obtained in this study with those of Redding for three values of the initial thrust to weight ratio. The agreement is exact to the accuracy obtained in reading Redding's values from curves. The transfer orbits associated with each case are presented in Table 3.

Table 2. Comparison with Selected Results of Redding

	Results of Current Study		Results of Redding
$(T/W)_o$	ΔV_T(ft/sec)	ΔV_{LOSS}(ft/sec)	ΔV_{LOSS}(ft/sec)
∞	13975.05	0.00	0.
0.500	14000.05	25.00	25.
0.250	14073.12	98.07	98.
0.125	14339.71	364.66	365.

where

ΔV_T = Total velocity increment required to perform transfer

ΔV_{LOSS} = Difference between a given ΔV_T and the impulsive ΔV_T

Table 3. Optimal Transfer Orbits to Geosynchronous Orbit

$(T/W)_o$	∞	0.500	0.250	0.125
INITIAL STATE:				
h_p(nmi)	119.784	119.784	119.784	119.784
h_a(nmi)	119.784	119.784	119.784	119.784
i(deg)	28.500	28.500	28.500	28.500
Ω(deg)	0.000	0.000	0.000	0.000
ω(deg)	0.000	0.000	0.000	0.000
ν(deg)	0.000	0.000	0.000	0.000
u(deg)	0.000	0.000	0.000	0.000
STATE AT 1^{st} BURN BURN-OUT:				
h_p(nmi)	119.784	135.320	182.165	372.479
h_a(nmi)	19364.385	19364.293	19364.022	19362.996
i(deg)	26.328	26.353	26.425	26.644
Ω(deg)	0.000	359.996	359.967	359.743
ω(deg)	0.000	0.000	359.998	359.987
ν(deg)	0.000	15.348	29.638	52.493
u(deg)	0.000	15.348	29.636	52.480
STATE AT 2^{nd} BURN BURN-OUT:				
h_p(nmi)	19364.384	19364.384	19364.384	19364.384
h_a(nmi)	19364.384	19364.384	19364.384	19364.384
i(deg)	0.000	0.000	0.000	0.000
Ω(deg)	0.000	0.000	0.000	0.000
ω(deg)	0.000	0.000	0.000	0.000
ν(deg)	180.000	180.327	180.625	180.020
u(deg)	180.000	180.327	180.625	180.020

Having established the validity of the optimization procedure, several problems involving larger plane changes were undertaken.

4.3 TRANSFERS BETWEEN A 28.5 DEGREE INCLINED CIRCULAR ORBIT AND 63.4 DEGREE INCLINED CIRCULAR ORBITS

4.3.1 Thrust-Limited Solutions

Circular orbits with inclinations of 63.4 degrees and altitudes between 300 and 10900 nmi have utility for both the military and civilian space programs [15, 35]. A complete investigation of the optimal transfers to these orbits from a 28.5 degree inclined, 150 nmi altitude circular orbit was undertaken by finding solutions for six values of final perigee altitude and five values of initial thrust to weight ratio $(T/W)_o$. The six final perigee altitudes chosen were 300, 800, 1250, 2500, 5000, and 10900 nmi. Four of the five values chosen for $(T/W)_o$ were ∞(i.e., infinity), 1.0, 0.1, and 0.05. The "fifth" value was different for each final orbit altitude but was approximately 0.04. This value was found to be the lowest value of $(T/W)_o$ for which the orbit transfers were optimal. Below this value it was not possible to find a solution of the assumed form which had the switching function positive during the first burn.

Tables 4 to 8 present the optimum values of the optimization variables, the corresponding values of the initial adjoint variables, the values of the final thrust to weight ratio $(T/W)_f$, the ratio of the final mass (or weight) to initial mass (or weight) m_f/m_o , and the total velocity increment imparted by the burns for the problems considered.

The following mnemonics are used in the tables to represent the optimization variables, adjoint variables, and total velocity increment:

$ACST_i$ - The i^{th} coast angle expressed in degrees.

$YVIH_i$ - The initial yaw angle in the VIH frame for the i^{th} burn; expressed in degrees.

$PVIH_i$ - The initial pitch angle in the VIH frame for the i^{th} burn; expressed in degrees.

$DYVIH_i$ - The time derivative of $YVIH_i$ expressed in degrees/second.

$DPVIH_i$ - The time derivative of $PVIH_i$ expressed in degrees/second.

$TBRN_i$ - The burn time for the i^{th} burn expressed in seconds.

$DLTV_i$ - The velocity increment imparted by the i^{th} burn; expressed in feet/second.

$AVRI_i$ - The i^{th} component of the scaled $\underline{\lambda}_r$ vector at the beginning of the first burn.

$AVVI_i$ - The i^{th} component of the scaled $\underline{\lambda}_v$ vector at the beginning of the first burn.

$DLTV_T$ - The total velocity increment imparted by all the burns during the transfer, i.e., the sum of the $DLTV_i$'s; expressed in feet/second.

The adjoint variables are expressed in normalized units, i.e., units in which lengths are scaled by the earth's radius and velocities are scaled by

Table 4. Values of Optimization Variables, Adjoint Variables, and Other Parameters for Optimal Thrust-Limited Transfers to 63.4 degree Inclined Circular Orbits with $(T/W)_o = \infty$

Final h_p(nmi)	300	800	1250	2500	5000	10900
$ACST_1$(deg)	0.000	0.000	0.000	0.000	0.000	0.000
$YVIH_1$(deg)	-53.311	-50.289	-47.557	-40.909	-29.697	-16.943
$PVIH_1$(deg)	0.000	0.000	0.000	0.000	0.000	0.000
$DLTV_1$(fps)	2531.021	2959.612	3286.145	4010.320	5260.549	6956.665
$ACST_2$(deg)	180.000	180.000	180.000	180.000	180.000	180.000
$YVIH_2$(deg)	101.949	97.913	94.915	88.803	79.338	66.885
$PVIH_2$(deg)	0.000	0.000	0.000	0.000	0.000	0.000
$DLTV_2$(fps)	9654.866	9450.997	9356.435	9255.154	8409.167	7174.575
$ACST_3$(deg)	180.000	180.000	180.000	180.000	-	-
$YVIH_3$(deg)	-128.992	-126.474	-125.004	-123.425	-	-
$PVIH_3$(deg)	0.000	0.000	0.000	-0.005	-	-
$DLTV_3$(fps)	2189.753	1615.965	1186.785	333.805	-	-
m_f/m_o	0.370498	0.379539	0.384744	0.390907	0.389010	0.376805
$DLTV_T$(fps)	14375.64	14026.57	13829.36	13599.28	13669.72	14131.24

Table 5. Values of Optimization Variables, Adjoint Variables, and Other Parameters for Optimal Thrust-Limited Transfers to 63.4 degree Inclined Circular Orbits with $(T/W)_o = 1.0$

Final h_p(nmi)	300	800	1250	2500	5000	10900
$ACST_1$(deg)	-2.503	-2.883	-3.171	-3.914	-4.842	-6.175
$YVIH_1$(deg)	-53.312	-50.258	-47.508	-40.831	-29.610	-16.865
$PVIH_1$(deg)	-0.360	-0.385	-0.408	-0.480	-0.665	-1.037
$DYVIH_1$(dps)	0.05750	0.05487	0.05240	0.04601	0.03421	0.01976
$DPVIH_1$(dps)	0.00962	0.00891	0.00859	0.00843	0.00916	0.11198
$TBRN_1$(sec)	72.943	83.669	91.691	108.964	137.101	171.760
$ACST_2$(deg)	173.244	173.497	173.648	173.850	173.843	173.047
$TBRN_2$(sec)	182.850	175.175	170.238	160.981	137.883	108.730
$ACST_3$(deg)	175.619	176.399	176.915	177.824	-	-
$TBRN_3$(sec)	27.586	20.445	15.004	4.197	-	-
$AVRI_1$	-0.76053	-0.84830	-0.91682	-1.05592	-1.22445	-1.31573
$AVRI_2$	0.01039	0.01642	0.02241	0.04110	0.07480	0.12682
$AVRI_3$	0.07266	0.08297	0.09027	0.10528	0.12064	0.12887
$AVVI_1$	-0.03550	-0.04560	-0.05420	-0.77560	-0.11072	-0.15214
$AVVI_2$	-0.25467	-0.34850	-0.43210	-0.63041	-0.94296	-1.25273
$AVVI_3$	-1.77284	-1.75657	-1.73765	-1.67500	-1.51909	-1.27145
$(T/W)_f$	2.700739	2.636032	2.600165	2.558886	2.571196	2.654703
m_f/m_o	0.370269	0.379358	0.384591	0.390795	0.388924	0.376690
$DLTV_T$(fps)	14384.58	14033.47	13835.12	13603.43	13672.91	14135.66

Table 6. Values of Optimization Variables, Adjoint Variables, and Other Parameters for Optimal Thrust-Limited Transfers to 63.4 degree Inclined Circular Orbits with $(T/W)_o$ = 0.1

Final h_p(nmi)	300	800	1250	2500	5000	10900
$ACST_1$(deg)	-33.515	-34.993	-36.385	-40.241	-48.254	-62.507
$YVIH_1$(deg)	-46.100	-42.423	-39.257	-31.958	-21.093	-8.668
$PVIH_1$(deg)	-4.453	-4.470	-4.604	-5.188	-6.519	-8.534
$DYVIH_1$(dps)	-0.00935	-0.01131	-0.01268	-0.01509	-0.01699	-0.01498
$DPVIH_1$(dps)	0.01065	0.01004	0.00977	0.00958	0.00949	0.00882
$TBRN_1$(sec)	959.324	1001.842	1041.964	1153.436	1384.000	1789.716
$ACST_2$(deg)	119.364	120.269	120.793	121.541	122.375	120.784
$TBRN_2$(sec)	1534.319	1524.562	1523.409	1520.889	1402.300	1061.387
$ACST_3$(deg)	142.465	148.808	153.031	160.401	-	-
$TBRN_3$(sec)	408.368	326.409	258.411	111.897	-	-
$AVRI_1$	-0.72091	-0.77644	-0.81058	-0.84578	-0.77998	-0.47254
$AVRI_2$	0.17561	0.24067	0.29946	0.44625	0.69862	1.04307
$AVRI_3$	1.00506	1.03090	1.05129	1.09538	1.14543	1.11396
$AVVI_1$	-0.56784	-0.64165	-0.70443	-0.85416	-1.10353	-1.43081
$AVVI_2$	-0.36081	-0.44463	-0.51400	-0.65679	-0.79938	-0.79036
$AVVI_3$	-1.66026	-1.61234	-1.56482	-1.43112	-1.16287	-0.73294
$(T/W)_f$	0.281604	0.273193	0.268462	0.262578	0.262590	0.272910
m_f/m_o	0.355109	0.366042	0.372492	0.380839	0.380822	0.366421
$DLTV_T$(fps)	14989.85	14550.82	14297.92	13977.06	13977.71	14535.83

Table 7. Values of Optimization Variables, Adjoint Variables, and Other Parameters for Optimal Thrust-Limited Transfers to 63.4 degree Inclined Circular Orbits with $(T/W)_o = 0.05$

Final h_p (nmi)	300	800	1250	2500	5000	10900
$ACST_1$ (deg)	-78.381	-80.078	-82.083	-89.024	-102.458	-134.926
$YVIH_1$ (deg)	-12.183	-9.833	-7.439	-0.797	8.185	16.238
$PVIH_1$ (deg)	-13.340	-12.241	-11.628	-11.000	-10.521	-7.324
$DYVIH_1$ (dps)	-0.05942	-0.05854	-0.05749	-0.05399	-0.04652	-0.02372
$DPVIH_1$ (dps)	0.01404	0.01124	0.00928	0.00555	0.00107	-0.00471
$TBRN_1$ (sec)	2235.688	2285.866	2345.497	2553.349	2961.518	3965.292
$ACST_2$ (deg)	71.985	73.614	74.734	76.985	81.132	95.148
$TBRN_2$ (sec)	2877.808	2830.138	2811.621	2813.622	2771.151	1934.468
$ACST_3$ (deg)	112.156	122.987	130.670	145.110	157.989	-
$TBRN_3$ (sec)	967.600	843.599	729.314	419.377	30.411	-
$AVRI_1$	0.07805	0.08563	0.11893	0.29275	0.66475	1.39175
$AVRI_2$	0.55737	0.62188	0.67815	0.79873	0.88623	0.73673
$AVRI_3$	2.21224	2.16200	2.11194	1.96655	1.69266	0.93168
$AVVI_1$	-1.58564	-1.63370	-1.67354	-1.75223	-1.77284	-1.36906
$AVVI_2$	-0.48183	-0.44734	-0.41648	-0.31500	-0.06983	0.67956
$AVVI_3$	-0.68020	-0.58308	-0.48463	-0.19886	0.24742	0.93430
$(T/W)_f$	0.154167	0.148007	0.144529	0.140027	0.139021	0.145150
m_f/m_o	0.324323	0.337822	0.345952	0.357073	0.359658	0.344471
$DLTV_T$ (fps)	16302.81	15712.40	15368.09	14909.99	14805.56	15430.20

Table 8. Values of Optimization Variables, Adjoint Variables, and Other Parameters for Optimal Thrust-Limited Transfers to 63.4 degree Inclined Circular Orbits with Minimum Values of $(T/W)_o$

Final h_p(nmi)	300	800	1250	2500	5000	10900
$(T/W)_o$	0.039275	0.039545	0.039829	0.040603	0.041002	0.034888
$ACST_1$(deg)	-115.633	-115.767	-116.458	-121.575	-136.653	-218.730
$YVIH_1$(deg)	29.937	28.076	27.038	27.042	30.749	19.434
$PVIH_1$(deg)	-15.650	-13.763	-12.423	-10.102	-7.147	2.572
$DYVIH_1$(dps)	-0.08004	-0.07398	-0.06882	-0.05600	-0.03605	0.01791
$DPVIH_1$(dps)	-0.00797	-0.00725	-0.00689	-0.00708	-0.00883	-0.00602
$TBRN_1$(sec)	3191.038	3206.186	3235.206	3401.788	3906.182	6277.786
$ACST_2$(deg)	55.633	58.008	59.983	64.945	73.074	96.627
$TBRN_2$(sec)	3533.960	3428.339	3359.261	3259.124	3143.186	2377.082
$ACST_3$(deg)	99.113	111.881	121.090	139.335	155.878	-
$TBRN_3$(sec)	1240.099	1099.073	973.443	604.222	94.277	-
$AVRI_1$	1.09902	1.06328	1.05056	1.11477	1.34629	1.40055
$AVRI_2$	0.28897	0.36830	0.42685	0.51538	0.50285	-0.68844
$AVRI_3$	2.07189	2.01078	1.93748	1.67238	1.13450	-0.88351
$AVVI_1$	-1.55676	-1.56782	-1.56674	-1.50279	-1.21063	1.11857
$AVVI_2$	-0.22535	-0.14153	-0.07256	0.10497	0.40818	0.82867
$AVVI_3$	0.85720	0.85497	0.86552	0.96937	1.25572	1.12746
$(T/W)_f$	0.128846	0.123429	0.120630	0.117867	0.117450	0.106041
m_f/m_o	0.304823	0.320387	0.330175	0.344482	0.349101	0.329006
$DLTV_T$(fps)	17200.59	16479.60	16043.90	15429.74	15236.90	16095.25

the circular orbital speed at one earth radius.

Tables 9 to 13 present the corresponding transfer orbits. These tables reveal that the first burn of a 3-burn transfer raises apogee; the second burn, performed near apogee, changes the inclination and raises perigee to the final orbit altitude; and the third burn lowers apogee to the final orbit altitude. A typical transfer is depicted in Figure 7. The transition from a 3-burn to a 2-burn solution occurs when the final orbit altitude is greater than or equal to the apogee altitude of the transfer orbit resulting from the first burn. Under these conditions, the necessity of the third "apogee lowering" burn is removed. Figure 8 attempts to summarize many of the pertinent characteristics of the problems considered.

Tables 4 to 8 reveal the similarity of the solutions for a given $(T/W)_o$. This similarity may suggest that using a solution for a given $(T/W)_o$ and a given final orbit altitude as an initial guess for a transfer to a different orbit altitude may be quite effective. This was indeed the case. Once one of the solutions for a given $(T/W)_o$ was obtained, all the rest were obtained quite quickly by using this solution as the initial guess.

To gain more insight into the nature of the finite burn orbit transfer, a "reverse" transfer from the 10900 nmi circular orbit to the 150 nmi circular orbit was flown for several values of $(T/W)_o$. The optimal solutions of these transfers are presented in Table 14 and the associated transfer orbits are presented in Table 15. Since the orbital rate during

Table 9. Transfer Orbits for Optimal Thrust-Limited Transfers to 63.4 degree Inclined Circular Orbits with $(T/W)_o = \infty$

Final h_p(nmi)	300	800	1250	2500	5000	10900
INITIAL STATE:						
h_p(nmi)	150.000	150.000	150.000	150.000	150.000	150.000
h_a(nmi)	150.000	150.000	150.000	150.000	150.000	150.000
i(deg)	28.500	28.500	28.500	28.500	28.500	28.500
Ω(deg)	0.000	0.000	0.000	0.000	0.000	0.000
ω(deg)	0.000	0.000	0.000	0.000	0.000	0.000
ν(deg)	0.000	0.000	0.000	0.000	0.000	0.000
u(deg)	0.000	0.000	0.000	0.000	0.000	0.000
STATE AT 1st BURN BURN-OUT:						
h_p(nmi)	150.000	150.000	150.000	150.000	150.000	150.000
h_a(nmi)	1215.123	1545.108	1851.908	2724.234	5000.000	10900.000
i(deg)	32.815	33.271	33.520	33.779	33.472	32.120
Ω(deg)	0.000	0.000	0.000	0.000	0.000	0.000
ω(deg)	0.000	0.000	0.000	0.000	0.000	0.000
ν(deg)	0.000	0.000	0.000	0.000	0.000	0.000
u(deg)	0.000	0.000	0.000	0.000	0.000	0.000
STATE AT 2nd BURN BURN-OUT:						
h_p(nmi)	300.000	800.000	1250.000	2500.000	5000.000	10900.000
h_a(nmi)	1215.123	1545.108	1851.908	2724.234	5000.000	10900.000
i(deg)	59.477	60.212	60.892	62.591	63.400	63.400
Ω(deg)	0.000	0.000	0.000	0.000	0.000	0.000
ω(deg)	0.000	0.003	359.999	359.995	0.000	0.000
ν(deg)	180.000	179.996	180.001	180.004	180.000	180.000
u(deg)	180.000	180.000	180.000	180.000	180.000	180.000
STATE AT 3rd BURN BURN-OUT:						
h_p(nmi)	300.000	800.000	1250.000	2500.000	-	-
h_a(nmi)	300.000	800.000	1250.000	2500.000	-	-
i(deg)	63.400	63.400	63.400	63.400	-	-
Ω(deg)	0.000	0.000	0.000	0.000	-	-
ω(deg)	0.000	0.000	0.000	0.000	-	-
ν(deg)	0.000	0.003	359.999	0.000	-	-
u(deg)	0.000	0.003	359.999	0.000	-	-

Table 10. Transfer Orbits for Optimal Thrust-Limited Transfers to 63.4 degree Inclined Circular Orbits with $(T/W)_o = 1.0$

Final h_p(nmi)	300	800	1250	2500	5000	10900
INITIAL STATE:						
h_p(nmi)	150.000	150.000	150.000	150.000	150.000	150.000
h_a(nmi)	150.000	150.000	150.000	150.000	150.000	150.000
i(deg)	28.500	28.500	28.500	28.500	28.500	28.500
Ω(deg)	0.000	0.000	0.000	0.000	0.000	0.000
ω(deg)	0.000	0.000	0.000	0.000	0.000	0.000
(deg)	0.000	0.000	0.000	0.000	0.000	0.000
u(deg)	0.000	0.000	0.000	0.000	0.000	0.000
STATE AT 1st BURN BURN-OUT:						
h_p(nmi)	150.098	150.168	150.241	150.478	151.150	152.568
h_a(nmi)	1230.071	1556.788	1861.451	2729.236	4999.741	10899.921
i(deg)	32.861	33.296	33.533	33.776	33.461	32.110
Ω(deg)	0.000	0.000	0.000	359.981	0.000	0.000
ω(deg)	359.998	359.998	359.999	359.899	0.000	359.999
ν(deg)	2.508	2.903	3.208	3.891	5.077	6.641
u(deg)	2.506	2.902	3.207	3.789	5.076	6.641
STATE AT 2nd BURN BURN-OUT:						
h_p(nmi)	300.011	800.003	1250.001	2500.000	5000.000	10900.000
h_a(nmi)	1230.145	1557.030	1861.776	2729.633	5000.000	10900.000
i(deg)	59.430	60.171	60.858	62.573	63.400	63.400
Ω(deg)	0.000	0.000	0.000	359.926	0.000	0.000
ω(deg)	0.002	0.001	0.001	359.937	0.000	0.000
ν(deg)	183.446	183.038	182.735	182.109	181.152	180.416
u(deg)	183.448	183.040	182.736	182.046	181.152	180.416
STATE AT 3rd BURN BURN-OUT:						
h_p(nmi)	300.000	800.000	1250.000	2500.000	-	-
h_a(nmi)	300.000	800.000	1250.000	2500.000	-	-
i(deg)	63.400	63.400	63.400	63.400	-	-
Ω(deg)	0.000	0.000	0.000	359.925	-	-
ω(deg)	0.000	0.000	0.000	0.000	-	-
ν(deg)	0.843	0.521	0.331	0.003	-	-
u(deg)	0.843	0.521	0.331	0.003	-	-

Table 11. Transfer Orbits for Optimal Thrust-Limited Transfers to 63.4 degree Inclined Circular Orbits with $(T/W)_o = 0.1$

Final h_p(nmi)	300	800	1250	2500	5000	10900
INITIAL STATE:						
h_p(nmi)	150.000	150.000	150.000	150.000	150.000	150.000
h_a(nmi)	150.000	150.000	150.000	150.000	150.000	150.000
i(deg)	28.500	28.500	28.500	28.500	28.500	28.500
Ω(deg)	0.000	0.000	0.000	0.000	0.000	0.000
ω(deg)	0.000	0.000	0.000	0.000	0.000	0.000
ν(deg)	0.000	0.000	0.000	0.000	0.000	0.000
u(deg)	0.000	0.000	0.000	0.000	0.000	0.000
STATE AT 1st BURN BURN-OUT:						
h_p(nmi)	175.919	182.368	188.840	209.075	264.066	412.192
h_a(nmi)	1884.997	2137.408	2385.255	3117.125	4972.407	10892.209
i(deg)	33.641	33.554	33.459	33.188	32.602	31.385
Ω(deg)	359.973	359.987	0.002	0.049	0.163	0.389
ω(deg)	359.227	359.289	359.337	359.438	359.508	359.269
ν(deg)	33.032	34.480	35.841	39.531	46.534	56.159
u(deg)	32.259	33.770	35.178	38.969	46.042	55.428
STATE AT 2nd BURN BURN-OUT:						
h_p(nmi)	303.772	801.392	1250.540	2500.026	5000.000	10900.000
h_a(nmi)	1890.701	2153.883	2408.502	3149.854	5000.000	10900.000
i(deg)	57.823	58.421	59.131	61.211	63.400	63.400
Ω(deg)	359.973	359.983	359.990	0.001	0.000	0.000
ω(deg)	0.405	0.293	0.212	0.041	0.000	0.000
ν(deg)	203.058	201.784	200.666	197.766	191.505	183.685
u(deg)	203.463	202.077	200.878	197.806	191.505	183.685
STATE AT 3rd BURN BURN-OUT:						
h_p(nmi)	300.000	800.000	1250.000	2500.000	-	-
h_a(nmi)	300.000	800.000	1250.000	2500.000	-	-
i(deg)	63.400	63.400	63.400	63.400	-	-
Ω(deg)	0.000	0.000	0.000	0 002	-	-
ω(deg)	0.000	0.000	0.000	0.000	-	-
ν(deg)	12.546	8.387	5.749	1.757	-	-
u(deg)	12.546	8.387	5.749	1.757	-	-

Table 12. Transfer Orbits for Optimal Thrust-Limited Transfers to 63.4 degree Inclined Circular Orbits with $(T/W)_o = 0.05$

Final h_p(nmi)	300	800	1250	2500	5000	10900
INITIAL STATE:						
h_p(nmi)	150.000	150.000	150.000	150.000	150.000	150.000
h_a(nmi)	150.000	150.000	150.000	150.000	150.000	150.000
i(deg)	28.500	28.500	28.500	28.500	28.500	28.500
Ω(deg)	0.000	0.000	0.000	0.000	0.000	0.000
ω(deg)	0.000	0.000	0.000	0.000	0.000	0.000
ν(deg)	0.000	0.000	0.000	0.000	0.000	0.000
u(deg)	0.000	0.000	0.000	0.000	0.000	0.000
STATE AT 1st BURN BURN-OUT:						
h_p(nmi)	338.123	359.630	383.110	463.734	643.303	1259.689
h_a(nmi)	2746.327	2892.607	3065.859	3679.756	5039.297	10875.915
i(deg)	32.219	32.137	32.045	31.789	31.485	31.378
Ω(deg)	0.470	0.522	0.588	0.835	1.379	2.597
ω(deg)	355.427	355.523	355.586	355.633	355.539	354.843
ν(deg)	69.542	70.196	71.031	73.812	77.777	79.448
u(deg)	64.969	65.719	66.617	69.445	73.316	74.291
STATE AT 2nd BURN BURN-OUT:						
h_p(nmi)	330.270	814.064	1256.818	2500.699	4999.993	10900.000
h_a(nmi)	2770.256	2944.749	3136.664	3779.584	5143.877	10900.000
i(deg)	57.360	57.165	57.370	59.132	63.000	63.400
Ω(deg)	0.004	0.011	0.021	0.036	0.007	0.000
ω(deg)	0.361	0.006	359.751	359.189	358.374	0.000
ν(deg)	213.270	212.316	211.321	208.255	202.523	184.876
u(deg)	213.631	212.321	211.072	207.444	200.897	184.876
STATE AT 3rd BURN BURN-OUT:						
h_p(nmi)	300.000	800.000	1250.000	2500.000	5000.000	-
h_a(nmi)	300.000	800.000	1250.000	2500.000	5000.000	-
i(deg)	63.400	63.400	63.400	63.400	63.400	-
Ω(deg)	0.000	0.000	0.000	0 000	0.000	-
ω(deg)	0.000	0.000	0.000	0.000	0.000	-
ν(deg)	28.819	20.905	15.526	6.020	359.452	-
u(deg)	28.819	20.905	15.526	6.020	359.452	-

Table 13. Transfer Orbits for Optimal Thrust-Limited Transfers to 63.4 degree Inclined Circular Orbits with Minimum Values of $(T/W)_o$

Final h_p(nmi)	300	800	1250	2500	5000	10900
$(T/W)_o$	.0392751	.0395451	.0398289	.0406026	.0410022	.0348875
INITIAL STATE:						
h_p(nmi)	150.000	150.000	150.000	150.000	150.000	150.000
h_a(nmi)	150.000	150.000	150.000	150.000	150.000	150.000
i(deg)	28.500	28.500	28.500	28.500	28.500	28.500
Ω(deg)	0.000	0.000	0.000	0.000	0.000	0.000
ω(deg)	0.000	0.000	0.000	0.000	0.000	0.000
ν(deg)	0.000	0.000	0.000	0.000	0.000	0.000
u(deg)	0.000	0.000	0.000	0.000	0.000	0.000
STATE AT 1^{st} BURN BURN-OUT:						
h_p(nmi)	558.261	581.982	607.852	708.840	985.408	2375.994
h_a(nmi)	3176.543	3259.555	3374.355	3891.336	5244.487	10871.374
i(deg)	31.816	31.810	31.796	31.764	31.900	34.063
Ω(deg)	1.828	1.814	1.834	2.058	2.968	3.180
ω(deg)	348.703	349.238	349.676	350.491	352.446	352.487
ν(deg)	85.916	85.449	85.165	85.084	85.467	76.910
u(deg)	74.619	74.686	74.841	75.574	77.913	69.397
STATE AT 2^{nd} BURN BURN-OUT:						
h_p(nmi)	356.269	827.641	1264.183	2501.578	4999.895	10900.000
h_a(nmi)	3190.278	3311.588	3451.225	4003.770	5358.159	10900.000
i(deg)	57.636	57.087	56.961	58.248	62.343	63.400
Ω(deg)	0.169	0.172	0.171	0.141	1.131	0.000
ω(deg)	358.426	358.034	357.768	357.165	357.088	0.000
ν(deg)	217.484	216.489	215.424	211.870	205.273	185.552
u(deg)	215.910	214.523	213.192	209.035	202.361	185.552
STATE AT 3^{rd} BURN BURN-OUT:						
h_p(nmi)	300.000	800.000	1250.000	2500.000	5000.000	-
h_a(nmi)	300.000	800.000	1250.000	2500.000	5000.000	-
i(deg)	63.400	63.400	63.400	63.400	63.400	-
Ω(deg)	0.000	0.000	0.000	0 000	1.113	-
ω(deg)	0.000	0.000	0.000	0.000	0.000	-
ν(deg)	35.156	25.806	19.520	7.880	0.000	-
u(deg)	35.156	25.806	19.520	7.880	0.000	-

Figure 7. Optimal Finite Three-Burn Transfer to a Circular Orbit for $(T/W)_o = 0.1$

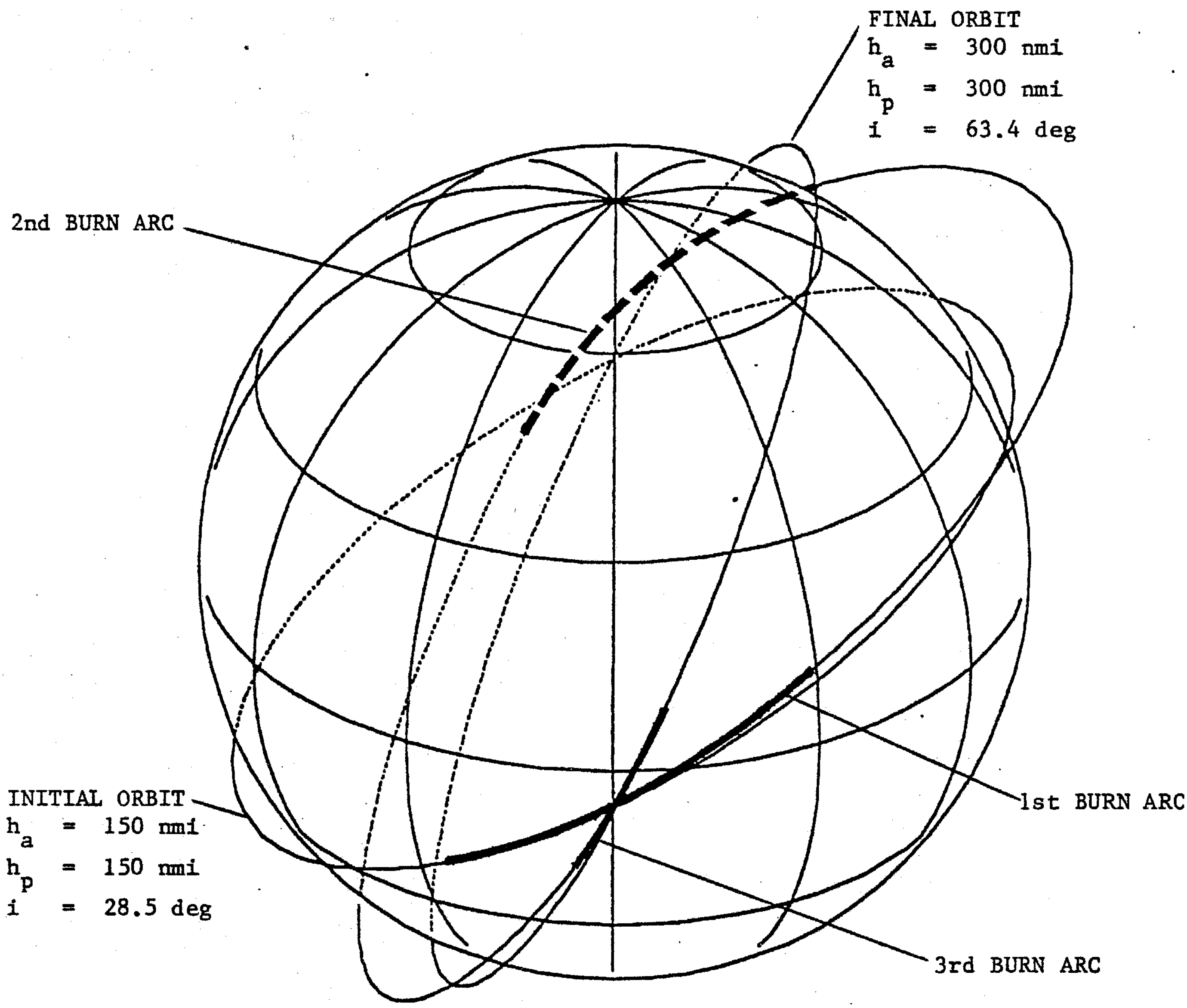

Figure 8. Propulsive ΔV Required for Transfers from a 28.5 Degree Inclined Circular Orbit to 63.4 Degree Inclined Circular Orbits

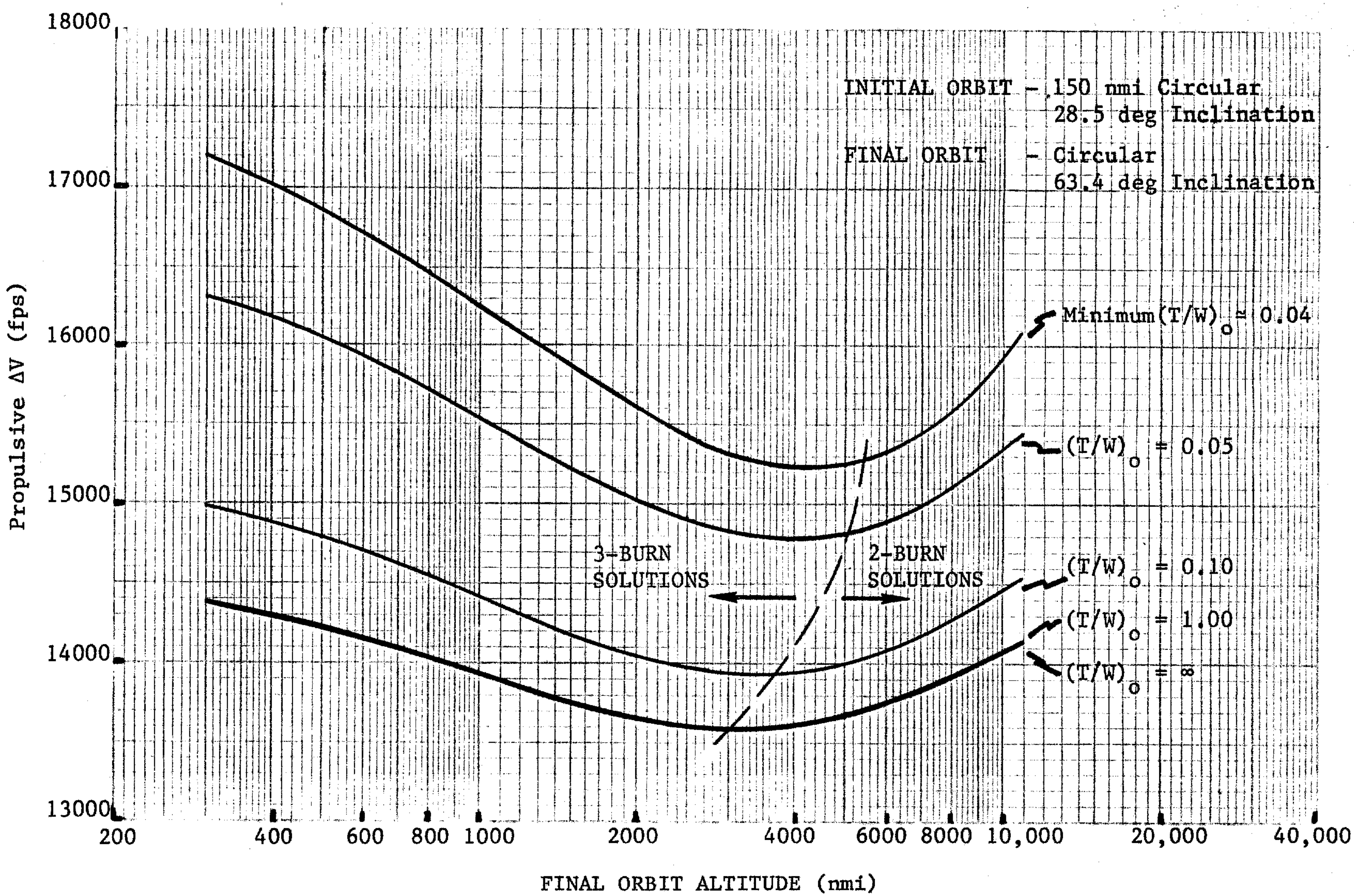

Table 14. Values of Optimization Variables, Adjoint Variables, and Other Parameters for Optimal Thrust-Limited Transfers from a 63.4 degree Inclined, 10900 nautical mile Altitude Circular Orbit

$(T/W)_o$	1.00	0.10	0.05	0.02
$ACST_1$(deg)	-0.795	-7.927	-15.764	-35.534
$YVIH_1$(deg)	144.386	143.583	141.453	126.845
$PVIH_1$(deg)	0.273	2.650	4.988	13.451
$DYVIH_1$(dps)	-0.08447	-0.00870	-0.00474	-0.00192
$DPVIH_1$(dps)	-0.00287	-0.00279	-0.00265	-0.00345
$TBRN_1$(sec)	175.849	1765.436	3560.477	8774.367
$ACST_2$(deg)	174.820	132.024	98.350	55.326
$TBRN_2$(sec)	104.610	1058.570	2186.686	6599.572
$AVRI_1$	0.09902	0.09795	0.09287	0.02840
$AVRI_2$	0.00046	0.00505	0.01276	0.06869
$AVRI_3$	-0.00289	-0.02878	-0.05701	-0.12445
$AVVI_1$	0.01168	0.11655	0.22929	0.26807
$AVVI_2$	-0.28067	-0.30617	-0.37398	-0.75757
$AVVI_3$	1.76923	1.76118	1.73685	1.60103
$(T/W)_f$	2.654217	0.268497	0.138341	0.063148
m_f/m_o	0.376759	0.372443	0.361426	0.316714
$DLTV_T$(fps)	14133.01	14299.82	14734.56	16646.54

Table 15. Transfer Orbits for Optimal Thrust-Limited Transfers from a 63.4 degree Inclined, 10900 nautical mile Altitude Circular Orbit

$(T/W)_o$	1.00	0.10	0.05	0.02
INITIAL STATE:				
h_p(nmi)	10900.000	10900.000	10900.000	10900.000
h_a(nmi)	10900.000	10900.000	10900.000	10900.000
i(deg)	63.400	63.400	63.400	63.400
Ω(deg)	0.000	0.000	0.000	0.000
ω(deg)	0.000	0.000	0.000	0.000
ν(deg)	0.000	0.000	0.000	0.000
u(deg)	0.000	0.000	0.000	0.000
STATE AT 1^{st} BURN BURN-OUT:				
h_p(nmi)	150.953	243.946	514.829	2508.994
h_a(nmi)	10899.792	10878.588	10809.266	10460.476
i(deg)	32.116	31.746	31.050	32.672
Ω(deg)	0.000	359.941	359.630	356.279
ω(deg)	180.000	180.119	180.780	191.479
ν(deg)	180.427	184.331	189.006	203.472
u(deg)	0.427	4.450	9.786	34.951
STATE AT 2^{nd} BURN BURN-OUT:				
h_p(nmi)	150.000	150.000	150.000	150.000
h_a(nmi)	150.000	150.000	150.000	150.000
i(deg)	28.500	28.500	28.500	28.500
Ω(deg)	0.000	0.000	0.000	0.000
ω(deg)	0.000	0.000	0.000	0.000
ν(deg)	183.206	211.715	242.282	351.499
u(deg)	183.206	211.715	242.282	351.499

the first burn is much lower for the reverse transfer than for the forward transfer, the burn arc for this burn is shorter for a given $(T/W)_o$ and consequently, the finite-burn losses are less.

4.3.2 Acceleration-Limited Solutions

During orbit transfers of some spacecraft, a requirement that the sensed acceleration not exceed a given upper bound may exist. A thrust-limited transfer has the characteristic that the acceleration reaches its maximum value at the conclusion of the last burn. An acceleration-limited transfer, however, has the characteristic that the acceleration can be maintained at a given upper bound for the duration of the burns. A comparison of the fuel efficiency for a thrust-limited and an acceleration-limited transfer to the 63.4 degree inclined, 300 nmi altitude circular orbit from the 28.5 degree inclined, 150 nmi altitude circular orbit is presented in Table 16. Both transfers maintain the acceleration below .1288 g's. The better fuel efficiency of the acceleration-limited transfer can be attributed to the shorter burn durations. Since the burns are performed at higher acceleration levels, less time is required to effect a given velocity change and consequently, finite burn losses are reduced.

4.4 TRANSFERS BETWEEN A 28.5 DEGREE INCLINED CIRCULAR ORBIT AND 63.4 DEGREE INCLINED ELLIPTICAL ORBITS

4.4.1 Thrust-Limited Solutions

Another class of orbits of interest to the space user community is the

Table 16. Comparison of Optimal Thrust-Limited and Acceleration-Limited Transfers to a 63.4 degree Inclined 300 nautical mile Altitude Circular Orbit

	Thrust Limited	Acceleration Limited
$(T/W)_o$	0.039275	0.128846
$ACST_1$(deg)	-115.633	-30.7417
$YVIH_1$(deg)	29.937	-45.569
$PVIH_1$(deg)	-15.650	-3.913
$DYVIH_1$(dps)	-0.08004	-0.00663
$DPVIH_1$(dps)	-0.00797	0.01015
$TBRN_1$(sec)	3191.038	912.261
$ACST_2$(deg)	55.633	118.236
$TBRN_2$(sec)	3533.960	1908.241
$ACST_3$(deg)	99.113	121.744
$TBRN_3$(sec)	1240.099	857.355
$AVRI_1$	1.09902	-0.76875
$AVRI_2$	0.28897	0.17931
$AVRI_3$	2.07189	0.90755
$AVVI_1$	-1.55676	-0.53448
$AVVI_2$	-0.22535	-0.39096
$AVVI_3$	0.85720	-1.66450
$(T/W)_f$	0.128846	0.128846
m_f/m_o	0.304823	0.348869
$DLTV_T$(fps)	17200.59	15246.52

	Thrust Limited	Acceleration Limited
	0.039275	0.128846
INITIAL STATE:		
h_p(nmi)	150.000	150.000
h_a(nmi)	150.000	150.000
i(deg)	28.500	28.500
Ω(deg)	0.000	0.000
ω(deg)	0.000	0.000
ν(deg)	0.000	0.000
u(deg)	0.000	0.000
STATE AT 1st BURN BURN-OUT:		
h_p(nmi)	558.261	176.184
h_a(nmi)	3176.543	2149.503
i(deg)	31.816	33.995
Ω(deg)	1.828	359.952
ω(deg)	348.703	359.164
ν(deg)	85.916	32.989
u(deg)	74.619	32.153
STATE AT 2nd BURN BURN-OUT:		
h_p(nmi)	356.269	318.971
h_a(nmi)	3190.278	2155.668
i(deg)	57.636	57.811
Ω(deg)	0.169	359.965
ω(deg)	358.426	0.807
ν(deg)	217.484	209.082
u(deg)	215.910	209.889
STATE AT 3rd BURN BURN-OUT:		
h_p(nmi)	300.000	300.000
h_a(nmi)	300.000	300.000
i(deg)	63.400	63.400
Ω(deg)	0.000	0.000
ω(deg)	0.000	0.000
ν(deg)	35.156	27.210
u(deg)	35.156	27.210

class of Molniya orbits, i.e., elliptical orbits with an inclination of 63.4 degrees, argument of perigee of 270 degrees, and a period of 12 hours [15,35]. A complete investigation of the optimal transfers to these orbits from a 28.5 degree inclined, 150 nmi altitude circular orbit was undertaken in a manner identical to that described in Section 4.3.1. The results of this investigation are presented in Tables 17 to 21.

Many of the comments made with regard to the transfers to the 63.4 degree inclined circular orbits also apply here. Tables 22 to 26 reveal that the first burn raises apogee and moves the argument of perigee; the second burn, performed near apogee, changes inclination and raises apogee an additional amount; and the third burn rotates the argument of perigee to 270 degrees and lowers apogee to its final value. A typical transfer is depicted in Figure 9. The transition from a 3-burn to a 2-burn solution occurs when the final apogee altitude is greater than or equal to the apogee altitude of the transfer orbit resulting from the second burn. Under these conditions, the necessity of the third "apogee lowering" burn is removed. The existence of the 3-burn solution is also probably due in large part to the value of the final argument of perigee. If this value were 0 or 180 degrees, only a 2-burn solution would be expected.

Figure 10 summarizes many of the pertinent characteristics of the transfers considered.

4.4.2 Acceleration-Limited Solutions

As in Section 4.3.2, a comparison of the fuel efficiency for a thrust-limited and an acceleration-limited transfer to the

Table 17. Values of Optimization Variables, Adjoint Variables, and Other Parameters for Optimal Thrust-Limited Transfers to Molniya Orbits with $(T/W)_o = \infty$

Final h_p(nmi)	300	800	1250	2500	5000	10900
$ACST_1$(deg)	249.748	247.126	244.625	237.123	220.553	180.000
$YVIH_1$(deg)	6.942	7.804	8.602	10.877	15.352	16.943
$PVIH_1$(deg)	-1.313	-1.447	-1.557	-1.817	-1.983	0.000
$DLTV_1$(fps)	8128.934	7993.087	7874.825	7549.388	6984.150	6956.665
$ACST_2$(deg)	151.918	152.169	152.604	154.401	160.078	180.000
$YVIH_2$(deg)	-86.484	-84.027	-82.162	-78.355	-74.172	-66.885
$PVIH_2$(deg)	13.094	12.902	12.646	11.747	9.155	0.000
$DLTV_2$(fps)	4569.653	4876.836	5147.560	5893.056	7171.690	7174.575
$ACST_3$(deg)	98.697	103.829	108.221	119.508	139.371	-
$YVIH_3$(deg)	139.043	138.095	137.497	136.456	134.760	-
$PVIH_3$(deg)	10.123	9.599	9.162	7.849	5.056	-
$DLTV_3$(fps)	2225.587	1957.301	1727.776	1128.716	151.892	-
m_f/m_o	0.356724	0.359120	0.361037	0.365528	0.372240	0.376805
$DLTV_T$(fps)	14924.17	14827.22	14750.16	14571.16	14307.73	14131.24

Table 18. Values of Optimization Variables, Adjoint Variables, and Other Parameters for Optimal Thrust-Limited Transfers to Molniya Orbits with $(T/W)_o = 1.0$

Final h_p (nmi)	300	800	1250	2500	5000	10900
$ACST_1$ (deg)	242.708	240.182	237.763	230.496	214.355	173.825
$YVIH_1$ (deg)	9.243	10.036	10.763	12.815	16.765	16.865
$PVIH_1$ (deg)	-3.115	-3.171	-3.216	-3.303	-3.184	-1.037
$DYVIH_1$ (dps)	-0.03328	-0.03387	-0.03432	-0.03526	-0.03562	-0.01976
$DPVIH_1$ (dps)	0.01704	0.01653	0.01609	0.01494	0.01290	0.11198
$TBRN_1$ (sec)	193.427	191.003	188.834	182.908	172.245	171.760
$ACST_2$ (deg)	144.052	144.401	144.902	146.946	153.017	173.047
$TBRN_2$ (sec)	69.511	74.122	78.258	89.379	108.580	108.730
$ACST_3$ (deg)	98.457	103.572	107.947	119.178	138.910	-
$TBRN_3$ (sec)	26.604	23.334	20.503	13.281	1.715	-
$AVRI_1$	0.64551	0.69711	0.74491	0.87847	1.11368	1.31573
$AVRI_2$	0.67523	0.66123	0.64568	0.58728	0.41186	-0.12682
$AVRI_3$	0.96099	0.93955	0.91596	0.83244	0.59993	-0.12887
$AVVI_1$	-1.61362	-1.57737	-1.53985	-1.41120	-1.04860	0.15214
$AVVI_2$	0.49832	0.54538	0.58962	0.71562	0.94698	1.25273
$AVVI_3$	0.59748	0.65081	0.70020	0.83993	1.10124	1.27145
$(T/W)_f$	2.804451	2.785678	2.770843	2.736689	2.687226	2.654703
m_f/m_o	0.356576	0.358979	0.360901	0.365405	0.372131	0.376690
$DLTV_T$ (fps)	14930.16	14832.92	14755.60	14576.04	14311.96	14135.66

Table 19. Values of Optimization Variables, Adjoint Variables, and Other Parameters for Optimal Thrust-Limited Transfers to Molniya Orbits with $(T/W)_o = 0.1$

Final h_p(nmi)	300	800	1250	2500	5000	10900
$ACST_1$(deg)	180.391	178.690	176.969	171.493	158.184	117.493
$YVIH_1$(deg)	24.780	24.759	24.654	24.085	21.685	8.668
$PVIH_1$(deg)	-14.385	-13.929	-13.539	-12.559	-10.849	-8.534
$DYVIH_1$(dps)	-0.01744	-0.01621	-0.01499	-0.01129	-0.00291	0.01498
$DPVIH_1$(dps)	0.01275	0.01230	0.01193	0.01108	0.00984	0.00882
$TBRN_1$(sec)	2032.391	1999.386	1969.742	1892.517	1780.804	1789.716
$ACST_2$(deg)	84.520	84.994	85.746	88.942	97.972	120.784
$TBRN_2$(sec)	697.716	747.975	793.705	915.234	1090.068	1061.387
$ACST_3$(deg)	94.630	99.835	104.246	115.320	-	-
$TBRN_3$(sec)	223.436	193.245	166.626	97.993	-	-
$AVRI_1$	1.34246	1.33558	1.32831	1.29969	1.19216	0.47254
$AVRI_2$	-0.36106	-0.37497	-0.39079	-0.44777	-0.60231	-1.04307
$AVRI_3$	-0.19074	-0.22136	-0.25324	-0.35705	-0.60479	-1.11396
$AVVI_1$	-0.45580	-0.39503	-0.33510	-0.14910	0.29455	1.43081
$AVVI_2$	1.03479	1.04840	1.06191	1.09757	1.13377	0.79036
$AVVI_3$	1.38944	1.39781	1.40325	1.40790	1.35531	0.73294
$(T/W)_f$	0.291044	0.288574	0.286637	0.282263	0.276222	0.272910
m_f/m_o	0.343591	0.346532	0.348873	0.354279	0.362028	0.366421
$DLTV_T$(fps)	15467.24	15343.84	15246.36	15023.73	14710.46	14535.83

Table 20. Values of Optimization Variables, Adjoint Variables, and Other Parameters for Optimal Thrust-Limited Transfers to Molniya Orbits with $(T/W)_o = 0.05$

Final h_p (nmi)	300	800	1250	2500	5000	10900
$ACST_1$ (deg)	112.269	111.794	110.997	106.996	91.738	45.074
$YVIH_1$ (deg)	11.554	11.397	11.014	8.855	0.839	-16.238
$PVIH_1$ (deg)	-13.083	-13.028	-12.894	-12.245	-10.241	-7.324
$DYVIH_1$ (dps)	0.02501	0.02548	0.02604	0.02815	0.03176	0.02372
$DPVIH_1$ (dps)	-0.00367	-0.00310	-0.00272	-0.00236	-0.00367	-0.00471
$TBRN_1$ (sec)	4579.015	4489.466	4401.700	4164.209	3923.497	3965.292
$ACST_2$ (deg)	50.904	49.520	48.985	50.967	64.218	95.148
$TBRN_2$ (sec)	1244.910	1348.297	1452.654	1749.431	2038.833	1934.468
$ACST_3$ (deg)	88.433	94.221	99.188	111.144	-	-
$TBRN_3$ (sec)	349.890	300.729	255.815	132.543	-	-
$AVRI_1$	0.37151	0.35142	0.32447	0.20402	-0.24229	-1.39175
$AVRI_2$	-1.29741	-1.28302	-1.27354	-1.26349	-1.25873	-0.73673
$AVRI_3$	-1.61539	-1.61727	-1.61923	-1.62705	-1.59205	-0.93168
$AVVI_1$	1.42836	1.43865	1.45701	1.54316	1.75219	1.36906
$AVVI_2$	0.73236	0.72318	0.70854	0.63507	0.31442	-0.67956
$AVVI_3$	0.79531	0.78509	0.76431	0.65146	0.20011	-0.93430
$(T/W)_f$	0.159225	0.157260	0.155719	0.152345	0.148140	0.145150
m_f/m_o	0.314021	0.317945	0.321092	0.328202	0.337519	0.344471
$DLTV_T$ (fps)	16770.17	16590.37	16447.77	16130.67	15725.39	15430.20

Table 21. Values of Optimization Variables, Adjoint Variables, and Other Parameters for Optimal Thrust-Limited Transfers to Molniya Orbits with Minimum Values of $(T/W)_o$

Final h_p(nmi)	300	800	1250	2500	5000	10900
$(T/W)_o$	0.039289	0.039052	0.038869	0.038684	0.039752	0.034888
$ACST_1$(deg)	66.729	65.673	64.585	60.912	51.094	-38.730
$YVIH_1$(deg)	-12.223	-12.963	-13.663	-15.603	-18.815	-19.434
$PVIH_1$(deg)	-2.679	-2.873	-3.044	-3.425	-3.526	2.572
$DYVIH_1$(dps)	0.03397	0.03435	0.03452	0.03392	0.02877	-0.01791
$DPVIH_1$(dps)	-0.01815	-0.01793	-0.01765	-0.01640	-0.01320	-0.00602
$TBRN_1$(sec)	6182.456	6133.645	6068.662	5782.381	5203.560	6277.786
$ACST_2$(deg)	47.921	45.284	43.390	42.449	56.350	96.627
$TBRN_2$(sec)	1436.667	1544.846	1661.021	2036.974	2448.622	2377.082
$ACST_3$(deg)	85.494	91.124	96.193	109.182	-	-
$TBRN_3$(sec)	438.686	384.465	334.747	192.550	-	-
$AVRI_1$	-0.90096	-0.93658	-0.97122	-1.07394	-1.28629	-1.40055
$AVRI_2$	-1.27203	-1.24362	-1.21551	-1.12804	-0.93622	0.68844
$AVRI_3$	-1.63094	-1.62283	-1.60919	-1.53530	-1.27098	0.88351
$AVVI_1$	1.63967	1.62571	1.61083	1.55710	1.38624	-1.11857
$AVVI_2$	-0.35883	-0.36780	-0.37848	-0.42413	-0.58362	-0.82867
$AVVI_3$	-0.62592	-0.65639	-0.68632	-0.77757	-0.97304	-1.12746
$(T/W)_f$	0.132516	0.130055	0.128100	0.124279	0.122680	0.106041
m_f/m_o	0.296483	0.300272	0.303426	0.311268	0.324030	0.329006
$DLTV_T$(fps)	17602.24	17418.38	17267.10	16897.66	16315.90	16095.25

Table 22. Transfer Orbits for Optimal Thrust-Limited Transfers to Molniya Orbits with $(T/W)_o = \infty$

Final h_p(nmi)	300	800	1250	2500	5000	10900
INITIAL STATE:						
h_p(nmi)	150.000	150.000	150.000	150.000	150.000	150.000
h_a(nmi)	150.000	150.000	150.000	150.000	150.000	150.000
i(deg)	28.500	28.500	28.500	28.500	28.500	28.500
Ω(deg)	0.000	0.000	0.000	0.000	0.000	0.000
ω(deg)	0.000	0.000	0.000	0.000	0.000	0.000
ν(deg)	0.000	0.000	0.000	0.000	0.000	0.000
u(deg)	0.000	0.000	0.000	0.000	0.000	0.000
STATE AT 1^{st} BURN BURN-OUT:						
h_p(nmi)	149.869	149.843	149.820	149.762	149.731	150.000
h_a(nmi)	20396.201	18885.538	17690.525	14885.262	11200.484	10900.000
i(deg)	29.121	29.272	29.424	29.916	31.069	32.120
Ω(deg)	3.243	3.518	3.740	4.188	4.150	0.000
ω(deg)	247.657	244.873	242.243	234.506	218.090	180.000
ν(deg)	359.249	359.173	359.110	358.961	358.860	0.000
u(deg)	246.906	244.046	241.353	233.467	216.950	180.000
STATE AT 2^{nd} BURN BURN-OUT:						
h_p(nmi)	2139.877	2497.471	2813.888	3645.255	5186.293	10900.000
h_a(nmi)	26585.727	25361.180	24323.041	21605.847	17060.829	10900.000
i(deg)	57.418	57.932	58.449	60.018	62.920	63.400
Ω(deg)	26.535	25.190	24.042	20.860	14.366	0.000
ω(deg)	248.350	250.497	252.299	257.203	267.694	270.000
ν(deg)	132.878	129.434	126.485	118.410	102.079	90.000
u(deg)	21.228	19.931	18.784	15.613	9.773	0.000
STATE AT 3^{rd} BURN BURN-OUT:						
h_p(nmi)	300.000	800.000	1250.000	2500.000	5000.000	-
h_a(nmi)	21500.000	21000.000	20550.000	19300.000	16800.000	-
i(deg)	63.400	63.400	63.400	63.400	63.400	-
Ω(deg)	15.807	16.539	16.989	17.153	14.045	-
ω(deg)	270.000	270.000	270.000	270.000	270.000	-
ν(deg)	215.241	218.009	220.439	226.879	239.288	-
u(deg)	125.241	128.009	130.439	136.879	149.288	-

Table 23. Transfer Orbits for Optimal Thrust-Limited Transfers to Molniya Orbits with $(T/W)_o = 1.0$

Final h_p(nmi)	300	800	1250	2500	5000	10900
INITIAL STATE:						
h_p(nmi)	150.000	150.000	150.000	150.000	150.000	150.000
h_a(nmi)	150.000	150.000	150.000	150.000	150.000	150.000
i(deg)	63.400	63.400	63.400	63.400	63.400	63.400
Ω(deg)	0.000	0.000	0.000	0.000	0.000	0.000
ω(deg)	0.000	0.000	0.000	0.000	0.000	0.000
ν(deg)	0.000	0.000	0.000	0.000	0.000	0.000
u(deg)	0.000	0.000	0.000	0.000	0.000	0.000
STATE AT 1st BURN BURN-OUT:						
h_p(nmi)	153.402	153.257	153.126	152.778	152.249	152.568
h_a(nmi)	20355.657	18851.780	17641.826	14859.458	11185.311	10899.921
i(deg)	29.142	29.291	29.441	29.928	31.071	32.110
Ω(deg)	3.214	3.488	3.709	4.157	4.123	0.000
ω(deg)	247.689	244.904	242.271	234.532	218.119	179.999
ν(deg)	6.920	6.728	6.561	6.130	5.526	6.641
u(deg)	254.609	251.632	248.831	240.662	223.645	186.641
STATE AT 2nd BURN BURN-OUT:						
h_p(nmi)	2135.833	2493.224	2807.731	3640.182	5180.843	10900.000
h_a(nmi)	26550.917	25332.915	24287.203	21588.062	17052.637	10900.000
i(deg)	57.424	57.936	58.461	60.026	62.933	63.400
Ω(deg)	26.474	25.132	23.975	20.811	14.340	0.000
ω(deg)	248.410	250.555	252.386	257.268	267.763	270.000
ν(deg)	132.964	129.549	126.581	118.615	102.454	90.416
u(deg)	21.375	20.104	18.968	15.882	10.217	0.416
STATE AT 3rd BURN BURN-OUT:						
h_p(nmi)	300.000	800.000	1250.000	2500.000	5000.000	-
h_a(nmi)	21500.000	21000.000	20550.000	19300.000	16800.000	-
i(deg)	63.400	63.400	63.400	63.400	63.400	-
Ω(deg)	15.748	16.481	16.929	17.110	14.028	-
ω(deg)	270.000	270.000	270.000	270.000	270.000	-
ν(deg)	215.273	218.041	220.452	226.894	239.280	-
u(deg)	125.273	128.041	130.452	136.894	149.280	-

Table 24. Transfer Orbits for Optimal Thrust-Limited Transfers to Molniya Orbits with $(T/W)_o = 0.1$

Final h_p(nmi)	300	800	1250	2500	5000	10900
INITIAL STATE:						
h_p(nmi)	150.000	150.000	150.000	150.000	150.000	150.000
h_a(nmi)	150.000	150.000	150.000	150.000	150.000	150.000
i(deg)	28.500	28.500	28.500	28.500	28.500	28.500
Ω(deg)	0.000	0.000	0.000	0.000	0.000	0.000
ω(deg)	0.000	0.000	0.000	0.000	0.000	0.000
ν(deg)	0.000	0.000	0.000	0.000	0.000	0.000
u(deg)	0.000	0.000	0.000	0.000	0.000	0.000
STATE AT 1st BURN BURN-OUT:						
h_p(nmi)	486.591	474.264	463.362	435.224	397.079	412.192
h_a(nmi)	18402.555	17000.449	15886.876	13436.343	10700.448	10892.209
i(deg)	30.758	30.707	30.673	30.665	30.954	31.385
Ω(deg)	0.136	0.397	0.634	1.232	1.816	0.389
ω(deg)	251.592	248.704	245.907	237.561	219.965	179.269
ν(deg)	60.440	59.741	59.110	57.440	55.056	56.159
u(deg)	312.031	308.445	305.017	295.001	275.021	235.428
STATE AT 2nd BURN BURN-OUT:						
h_p(nmi)	1869.185	2197.963	2494.873	3311.752	5000.000	10900.000
h_a(nmi)	24718.402	23715.564	22854.406	20616.124	16800.000	10900.000
i(deg)	57.770	58.272	58.822	60.542	63.400	63.400
Ω(deg)	22.143	20.850	19.807	17.205	12.253	0.000
ω(deg)	252.109	254.392	256.319	261.245	270.000	270.000
ν(deg)	131.619	128.055	125.033	117.406	104.364	93.685
u(deg)	23.728	22.447	21.352	18.651	14.364	3.685
STATE AT 3rd BURN BURN-OUT:						
h_p(nmi)	300.000	800.000	1250.000	2500.000	-	-
h_a(nmi)	21500.000	21000.000	20550.000	19300.000	-	-
i(deg)	63.400	63.400	63.400	63.400	-	-
Ω(deg)	11.628	12.429	13.047	13.970	-	-
ω(deg)	270.000	270.000	270.000	270.000	-	-
ν(deg)	214.538	217.315	219.703	226.045	-	-
u(deg)	124.538	127.315	129.703	136.045	-	-

Table 25. Transfer Orbits for Optimal Thrust-Limited Transfers to Molniya Orbits with $(T/W)_o = 0.05$

Final h_p(nmi)	300	800	1250	2500	5000	10900
INITIAL STATE:						
h_p(nmi)	150.000	150.000	150.000	150.000	150.000	150.000
h_a(nmi)	150.000	150.000	150.000	150.000	150.000	150.000
i(deg)	28.500	28.500	28.500	28.500	28.500	28.500
Ω(deg)	0.000	0.000	0.000	0.000	0.000	0.000
ω(deg)	0.000	0.000	0.000	0.000	0.000	0.000
ν(deg)	0.000	0.000	0.000	0.000	0.000	0.000
u(deg)	0.000	0.000	0.000	0.000	0.000	0.000
STATE AT 1st BURN BURN-OUT:						
h_p(nmi)	1417.291	1372.579	1332.287	1232.465	1165.277	1259.689
h_a(nmi)	17734.441	16270.693	15066.971	12518.579	10650.447	10875.915
i(deg)	34.148	33.760	33.333	32.103	30.679	31.378
Ω(deg)	355.065	355.174	355.354	356.245	358.708	2.597
ω(deg)	260.566	257.957	255.077	245.181	222.875	174.843
ν(deg)	84.830	84.686	84.409	83.203	80.816	79.448
u(deg)	345.396	342.643	339.486	328.385	303.692	259.448
STATE AT 2nd BURN BURN-OUT:						
h_p(nmi)	1674.709	1945.011	2203.812	3000.764	5000.000	10900.000
h_a(nmi)	23245.827	22403.594	21690.978	19876.532	16800.000	10900.000
i(deg)	58.405	58.761	59.237	61.052	63.400	63.400
Ω(deg)	16.186	14.745	13.700	11.779	8.925	0.000
ω(deg)	255.571	257.975	259.989	264.771	270.000	270.000
ν(deg)	132.831	128.949	125.655	117.941	107.768	94.876
u(deg)	28.403	26.924	25.644	22.713	17.768	4.876
STATE AT 3rd BURN BURN-OUT:						
h_p(nmi)	300.000	800.000	1250.000	2500.000	-	-
h_a(nmi)	21500.000	21000.000	20550.000	19300.000	-	-
i(deg)	63.400	63.400	63.400	63.400	-	-
Ω(deg)	6.322	6.837	7.408	9.113	-	-
ω(deg)	270.000	270.000	270.000	270.000	-	-
ν(deg)	213.100	216.333	219.089	225.835	-	-
u(deg)	123.100	126.333	129.089	135.835	-	-

Table 26. Transfer Orbits for Optimal Thrust-Limited Transfers to Molniya Orbits with Minimum Values of $(T/W)_o$

Final h_p(nmi)	300	800	1250	2500	5000	10900
$(T/W)_o$	.0392889	.0390523	.0388693	.0386836	.0397516	.0348875
INITIAL STATE:						
h_p(nmi)	150.000	150.000	150.000	150.000	150.000	150.000
h_a(nmi)	150.000	150.000	150.000	150.000	150.000	150.000
i(deg)	28.500	28.500	28.500	28.500	28.500	28.500
Ω(deg)	0.000	0.000	0.000	0.000	0.000	0.000
ω(deg)	0.000	0.000	0.000	0.000	0.000	0.000
ν(deg)	0.000	0.000	0.000	0.000	0.000	0.000
u(deg)	0.000	0.000	0.000	0.000	0.000	0.000
STATE AT 1^{st} BURN BURN-OUT:						
h_p(nmi)	2144.869	2106.559	2067.533	1941.912	1744.947	2375.994
h_a(nmi)	18528.089	17099.045	15855.145	12972.219	10557.061	10871.374
i(deg)	35.145	34.907	34.567	33.126	31.075	34.063
Ω(deg)	354.583	354.609	354.700	355.501	358.839	3.180
ω(deg)	262.705	260.742	258.435	248.907	223.933	172.487
ν(deg)	85.739	86.116	86.320	85.926	83.252	76.910
u(deg)	348.444	346.859	344.754	334.833	307.186	249.397
STATE AT 2^{nd} BURN BURN-OUT:						
h_p(nmi)	1896.774	2140.025	2366.998	3093.036	5000.000	10900.000
h_a(nmi)	23247.380	22394.192	21667.692	19865.256	16800.000	10900.000
i(deg)	58.576	58.799	59.131	60.639	63.400	63.400
Ω(deg)	15.336	13.692	12.418	10.083	7.843	0.000
ω(deg)	254.533	256.941	259.025	264.033	270.000	270.000
ν(deg)	134.958	131.184	127.846	119.681	108.533	95.552
u(deg)	29.492	28.125	26.871	23.713	18.533	5.552
STATE AT 3^{rd} BURN BURN-OUT:						
h_p(nmi)	300.000	800.000	1250.000	2500.000	-	-
h_a(nmi)	21500.000	21000.000	20550.000	19300.000	-	-
i(deg)	63.400	63.400	63.400	63.400	-	-
Ω(deg)	5.165	5.349	5.607	6.869	-	-
ω(deg)	270.000	270.000	270.000	270.000	-	-
ν(deg)	211.672	214.952	217.900	225.460	-	-
u(deg)	121.672	124.952	127.900	135.460	-	-

Figure 9. Optimal Finite Three-Burn Transfer to an Elliptical Orbit for $(T/W)_o = 0.1$

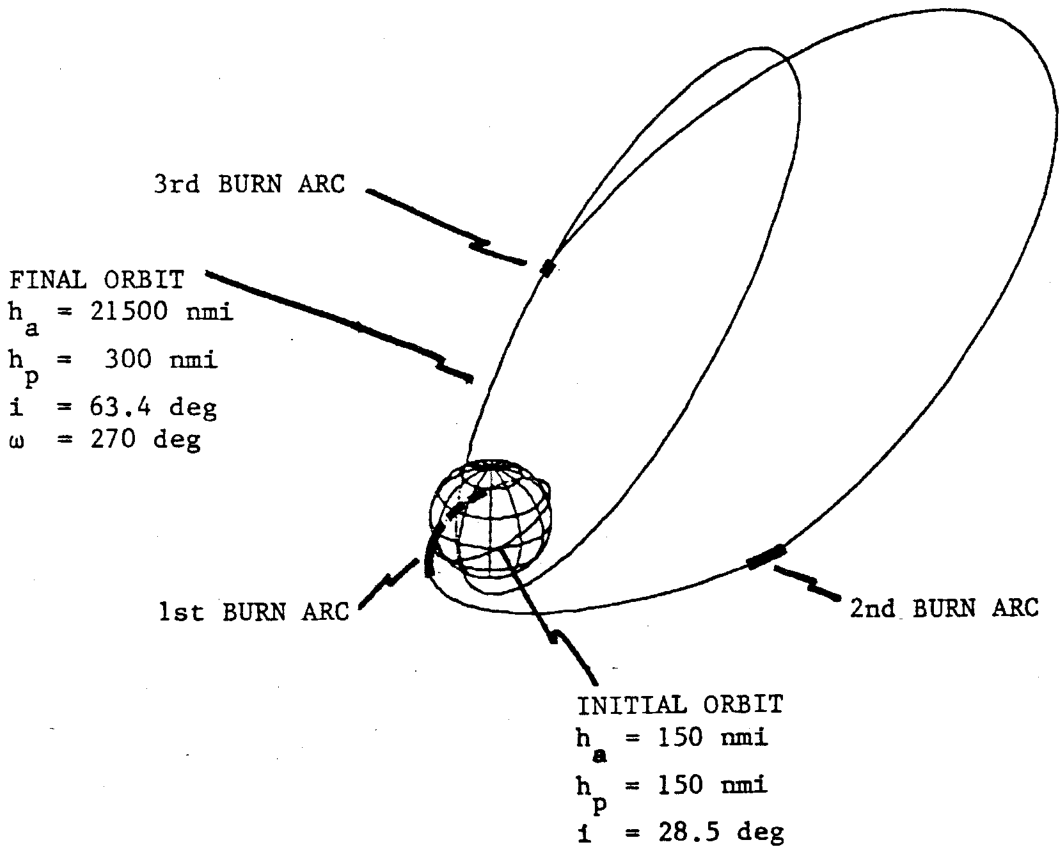

Figure 10. Propulsive ΔV Required for Transfers from a 28.5 Degree Inclined Circular Orbit to 63.4 Degree Inclined Elliptical Orbits

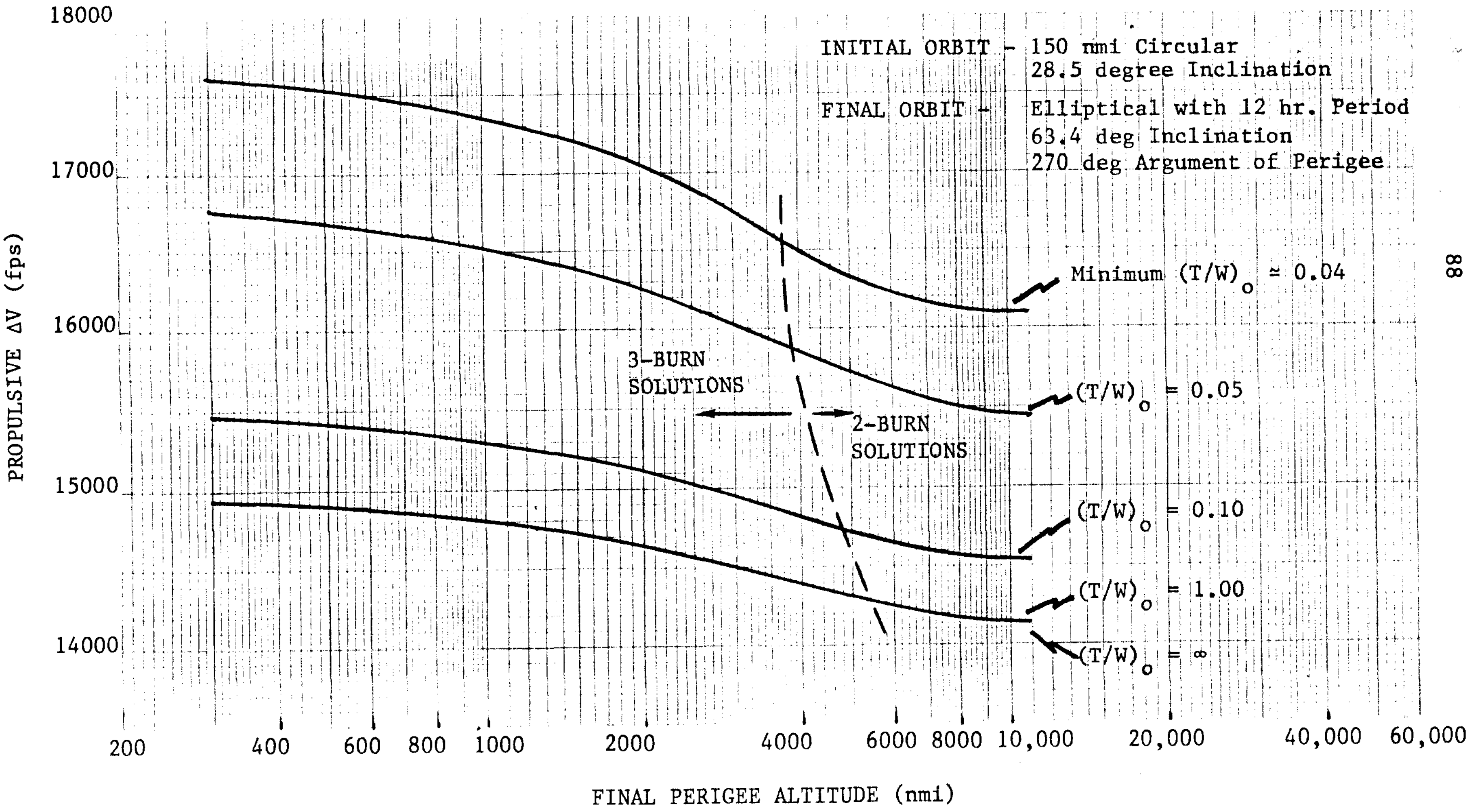

63.4 degree inclined, 300 nmi perigee altitude elliptical orbit from the 28.5 degree inclined, 150 nmi altitude circular orbit was made. The results are presented in Table 27. Note that both transfers maintain the acceleration at or below .1325 g's. As found with the comparison described in Section 4.3.2, the acceleration-limited transfer is more fuel efficient.

4.5 TRANSFERS BETWEEN 97 DEGREE INCLINED CIRCULAR ORBITS AND A 57 DEGREE INCLINED CIRCULAR ORBIT

Besides the orbit transfers to 63.4 degree inclined orbits, other orbit transfers of interest requiring large plane changes are transfers from 97 degree inclined circular (i.e., near sun-synchronous) orbits to a 57 degree inclined, 150 nmi altitude circular orbit [35]. Since the altitude range of interest is not as large as that for the previous cases, only altitudes of 900 and 1500 nmi were considered. The 3-burn solutions for four values of $(T/W)_o$ are presented in Tables 28 and 29. The corresponding transfer orbits are presented in Tables 30 and 31. For the values of altitude and $(T/W)_o$ considered, we observe that all the solutions are 3-burn solutions. Again, a lower limit for $(T/W)_o$ was discovered, below which no optimal transfers were found.

The pertinent characteristics of these transfers are depicted in Figure 11.

Table 27. Comparison of Optimal Thrust-Limited and Acceleration-Limited Transfers to a 300 nautical mile Perigee Altitude Molniya Orbit

	Thrust Limited	Acceleration Limited
$(T/W)_o$	0.039289	0.132516
$ACST_1$(deg)	66.729	187.640
$YVIH_1$(deg)	-12.223	22.714
$PVIH_1$(deg)	-2.679	-12.988
$DYVIH_1$(dps)	0.03397	-0.01867
$DPVIH_1$(dps)	-0.01815	0.01325
$TBRN_1$(sec)	6182.456	2029.063
$ACST_2$(deg)	47.921	78.000
$TBRN_2$(sec)	1436.667	1142.054
$ACST_3$(deg)	85.494	92.951
$TBRN_3$(sec)	438.686	452.795
$AVRI_1$	-0.90096	1.35901
$AVRI_2$	-1.27203	-0.21515
$AVRI_3$	-1.63094	-0.02032
$AVVI_1$	1.63967	-0.61310
$AVVI_2$	-0.35883	1.03385
$AVVI_3$	-0.62592	1.32829
$(T/W)_f$	0.132516	0.132516
m_f/m_o	0.296483	0.343980
$DLTV_T$(fps)	17602.24	15450.87

	Thrust Limited	Acceleration Limited
	0.039289	0.132516
INITIAL STATE:		
h_p(nmi)	150.000	150.000
h_a(nmi)	150.000	150.000
i(deg)	28.500	28.500
Ω(deg)	0.000	0.000
ω(deg)	0.000	0.000
ν(deg)	0.000	0.000
u(deg)	0.000	0.000
STATE AT 1st BURN BURN-OUT:		
h_p(nmi)	2144.869	479.788
h_a(nmi)	18528.089	18102.024
i(deg)	35.145	30.795
Ω(deg)	354.583	0.247
ω(deg)	262.705	251.250
ν(deg)	85.739	65.666
u(deg)	348.444	316.915
STATE AT 2nd BURN BURN-OUT:		
h_p(nmi)	1896.774	1854.902
h_a(nmi)	23247.380	24573.193
i(deg)	58.576	57.829
Ω(deg)	15.336	21.901
ω(deg)	254.533	252.403
ν(deg)	134.958	132.322
u(deg)	29.492	24.725
STATE AT 3rd BURN BURN-OUT:		
h_p(nmi)	300.000	300.000
h_a(nmi)	21500.000	21500.000
i(deg)	63.400	63.400
Ω(deg)	5.165	11.426
ω(deg)	270.000	270.000
ν(deg)	211.672	214.836
u(deg)	121.672	124.836

Table 28. Values of Optimization Variables, Adjoint Variables, and Other Parameters for Optimal Thrust-Limited Transfers from "Sun-Synchronous" Orbit with $(T/W)_o$ = 1.0 and $(T/W)_o$ = 0.1

	$(T/W)_o = 1.0$		$(T/W)_o = 0.1$	
Initial h_p(nmi)	900	1500	900	1500
$ACST_1$(deg)	-1.567	-0.999	-21.918	-14.982
$YVIH_1$(deg)	50.400	51.146	46.066	48.520
$PVIH_1$(deg)	-0.309	-0.218	-4.153	-3.070
$DYVIH_1$(dps)	-0.06125	-0.06621	-0.00090	-0.00421
$DPVIH_1$(dps)	0.00992	0.00904	0.01051	0.00913
$TBRN_1$(sec)	60.996	47.468	837.249	697.524
$ACST_2$(deg)	174.934	175.787	134.809	142.886
$TBRN_2$(sec)	194.233	198.176	1672.680	1721.832
$ACST_3$(deg)	175.777	175.792	142.329	141.620
$TBRN_3$(sec)	41.961	48.221	505.440	555.960
$AVRI_1$	-0.55550	-0.42516	-0.55732	-0.44017
$AVRI_2$	0.02377	0.01265	0.32337	0.18557
$AVRI_3$	0.02511	0.01302	0.36510	0.19965
$AVVI_1$	-0.02155	-0.01277	-0.34236	-0.21361
$AVVI_2$	-1.23085	-1.24767	-1.13102	-1.18766
$AVVI_3$	-1.30139	-1.28539	-1.34635	-1.32397
$(T/W)_f$	2.944822	2.882127	0.303106	0.295143
m_f/m_o	0.339579	0.346966	0.329918	0.338819
$DLTV_T$(fps)	15637.29	15325.72	16055.17	15669.75

Table 29. Values of Optimization Variables, Adjoint Variables, and Other Parameters for Optimal Thrust-Limited Transfers from "Sun-Synchronous" Orbit with $(T/W)_o = 0.05$ and Minimum Values of $(T/W)_o$

	$(T/W)_o = 0.05$		$(T/W)_o =$ .0267748	.0210557
Initial h_p(nmi)	900	1500	900	1500
$ACST_1$(deg)	-52.115	-37.330	-129.598	-127.501
$YVIH_1$(deg)	30.846	39.841	-42.280	-41.946
$PVIH_1$(deg)	-11.100	-8.143	-17.735	-18.784
$DYVIH_1$(dps)	0.01627	0.00522	0.05311	0.04666
$DPVIH_1$(dps)	0.01425	0.01108	-0.01158	-0.00926
$TBRN_1$(sec)	1989.165	1731.256	4765.542	5708.635
$ACST_2$(deg)	96.789	111.316	52.525	50.142
$TBRN_2$(sec)	3095.147	3146.005	5407.190	6922.722
$ACST_3$(deg)	111.230	109.658	72.646	53.893
$TBRN_3$(sec)	1119.307	1216.676	2146.354	3129.870
$AVRI_1$	-0.33808	-0.37791	1.04225	0.84722
$AVRI_2$	0.71032	0.44224	0.89240	0.78509
$AVRI_3$	0.92446	0.53160	0.77010	0.65374
$AVVI_1$	-0.97936	-0.62391	-1.32054	-1.35190
$AVVI_2$	-0.74847	-0.97694	1.09252	1.08737
$AVVI_3$	-1.29989	-1.36580	0.52119	0.44617
$(T/W)_f$	0.160922	0.154849	0.100272	0.080205
m_f/m_o	0.310709	0.322896	0.267021	0.262525
$DLTV_T$(fps)	16923.69	16366.67	19117.59	19363.45

Table 30. Transfer Orbits for Optimal Thrust-Limited Transfers from "Sun-Synchronous" Orbit with $(T/W)_o = 1.0$ and $(T/W)_o = 0.1$

	$(T/W)_o = 1.0$		$(T/W)_o = 0.1$	
Initial h_p(nmi)	900	1500	900	1500
INITIAL STATE:				
h_p(nmi)	900.000	1500.000	900.000	1500.000
h_a(nmi)	900.000	1500.000	900.000	1500.000
i(deg)	97.000	97.000	97.000	97.000
Ω(deg)	0.000	0.000	0.000	0.000
ω(deg)	0.000	0.000	0.000	0.000
ν(deg)	0.000	0.000	0.000	0.000
u(deg)	0.000	0.000	0.000	0.000
STATE AT 1st BURN BURN-OUT:				
h_p(nmi)	900.041	1500.015	912.083	1505.186
h_a(nmi)	2138.198	2587.692	2954.512	3387.076
i(deg)	93.196	93.825	92.155	92.531
Ω(deg)	0.000	0.000	0.016	0.013
ω(deg)	359.999	359.999	359.612	359.720
ν(deg)	1.582	1.009	22.018	15.102
u(deg)	1.581	1.008	21.630	14.823
STATE AT 2nd BURN BURN-OUT:				
h_p(nmi)	150.055	150.086	160.237	163.884
h_a(nmi)	2137.936	2587.302	2940.357	3364.296
i(deg)	62.040	62.218	62.449	62.370
Ω(deg)	0.000	0.000	0.021	0.017
ω(deg)	0.001	0.001	0.296	0.267
ν(deg)	182.619	182.329	197.855	196.377
u(deg)	182.620	182.330	198.151	196.644
STATE AT 3rd BURN BURN-OUT:				
h_p(nmi)	150.000	150.000	150.000	150.000
h_a(nmi)	150.000	150.000	150.000	150.000
i(deg)	57.000	57.000	57.000	57.000
Ω(deg)	0.000	0.000	0.000	0.000
ω(deg)	0.000	0.000	0.000	0.000
ν(deg)	1.342	1.535	16.211	17.717
u(deg)	1.342	1.535	16.211	17.717

Table 31. Transfer Orbits for Optimal Thrust-Limited Transfers from "Sun-Synchronous" Orbit with $(T/W)_o = 0.05$ and Minimum Values of $(T/W)_o$

	$(T/W)_o = 0.05$	$(T/W)_o = 0.05$	$(T/W)_o =$ .0267748	$(T/W)_o =$ .0210557
Initial h_p(nmi)	900	1500	900	1500
INITIAL STATE:				
h_p(nmi)	900.000	1500.000	900.000	1500.000
h_a(nmi)	900.000	1500.000	900.000	1500.000
i(deg)	97.000	97.000	97.000	97.000
Ω(deg)	0.000	0.000	0.000	0.000
ω(deg)	0.000	0.000	0.000	0.000
ν(deg)	0.000	0.000	0.000	0.000
u(deg)	0.000	0.000	0.000	0.000
STATE AT 1^{st} BURN BURN-OUT:				
h_p(nmi)	992.716	1545.414	1524.579	2179.297
h_a(nmi)	3953.650	4371.282	5321.217	6477.947
i(deg)	92.689	92.304	93.862	93.820
Ω(deg)	359.959	0.011	358.685	358.698
ω(deg)	358.428	359.063	349.970	349.712
ν(deg)	50.397	37.213	142.281	89.938
u(deg)	48.825	36.276	132.250	79.651
STATE AT 2^{nd} BURN BURN-OUT:				
h_p(nmi)	210.203	226.484	398.703	685.528
h_a(nmi)	3922.856	4315.208	5232.341	6287.977
i(deg)	62.009	61.754	60.657	59.707
Ω(deg)	0.003	359.991	359.728	359.493
ω(deg)	0.768	0.858	359.245	0.755
ν(deg)	205.739	203.829	215.014	216.700
u(deg)	206.507	204.688	214.259	217.456
STATE AT 3^{rd} BURN BURN-OUT:				
h_p(nmi)	150.000	150.000	150.000	150.000
h_a(nmi)	150.000	150.000	150.000	150.000
i(deg)	57.000	57.000	57.000	57.000
Ω(deg)	0.002	0.000	0.000	0.000
ω(deg)	0.000	0.000	0.000	0.000
ν(deg)	35.215	38.096	62.161	87.484
u(deg)	35.215	38.096	62.161	87.484

Figure 11. Propulsive ΔV Required for Transfers from 97 Degree Inclined Circular Orbits to a 57 Degree Inclined Circular Orbit

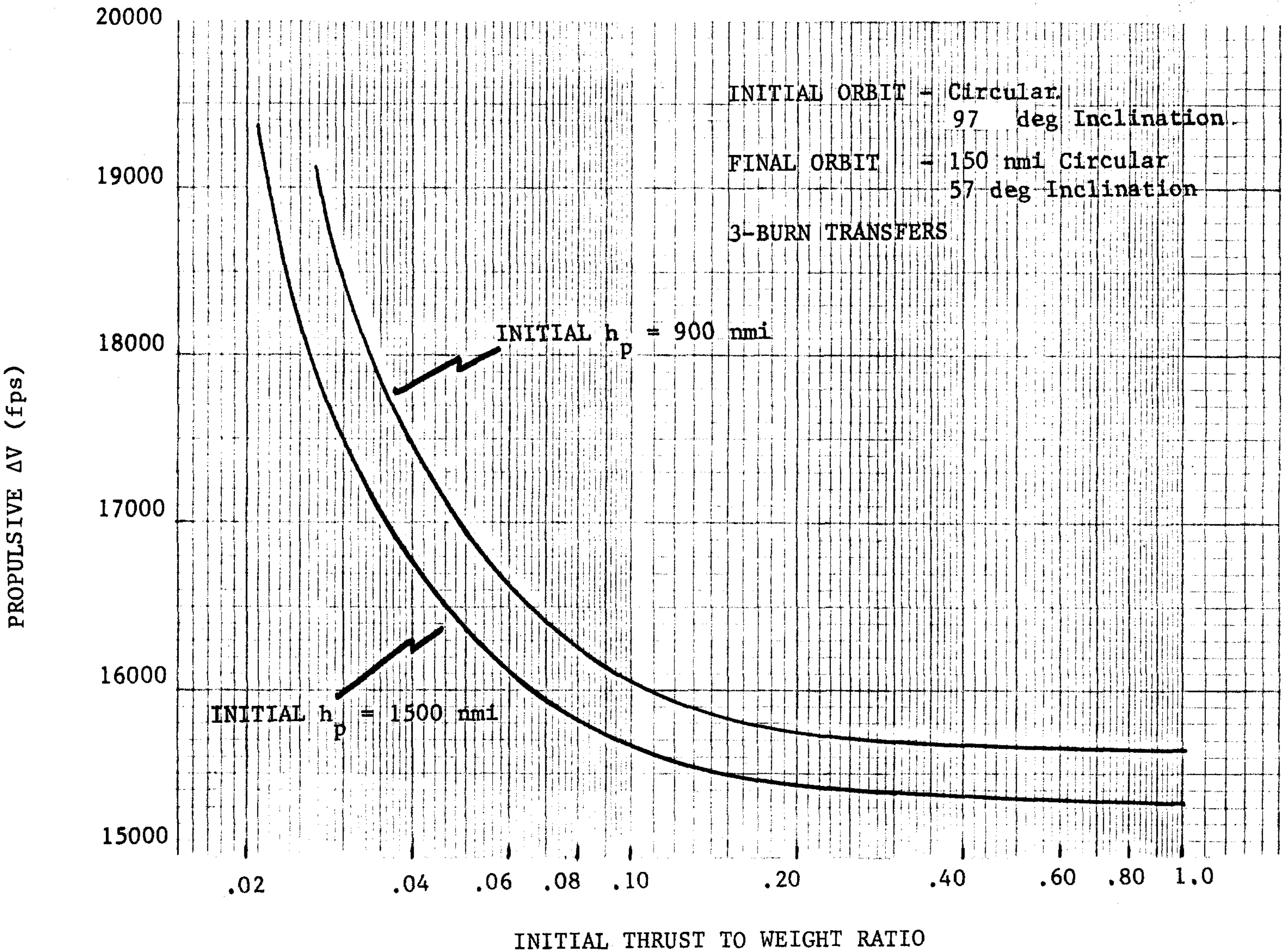

4.6 ANALYSIS OF THRUST POINTING ANGLES

A qualitative analysis of the thrust pointing angles was undertaken to determine the similarity of the optimal pointing angle time history to simple types of control laws, i.e., control laws where the pointing angles vary linearly or are constant with time. Previous authors [14, 15] have suggested that some of these simple control laws closely approximate the optimal control. These previous studies did not, however, investigate the effect of the pointing angle coordinate system on the "optimality" of these simple control laws. With regard to the coordinate systems depicted in Figures 1, 4, and 5, it seems reasonable to suspect that the time histories of the pointing angles in these different systems may be more or less "simple".

The analysis was carried out by making plots of the changes in the pointing angles during the burns of three different orbit transfers. For each burn, three plots were made, each corresponding to the three coordinate systems of Figures 1, 4, and 5. The transfers chosen were those from the 28.5 degree inclined, low altitude circular orbit to the geosynchronous orbit, the 63.4 degree inclined, 300 nmi altitude circular orbit, and the 300 nmi perigee altitude Molniya orbit. In order to make the best possible comparison with the previous studies, an initial thrust to weight ratio of 0.1 and a specific impulse of 300 sec was used. The resulting plots are presented in Figures 12 to 14.

Figure 12. Changes in Thrust Pointing Angles for Transfer to Geosynchronous Orbit

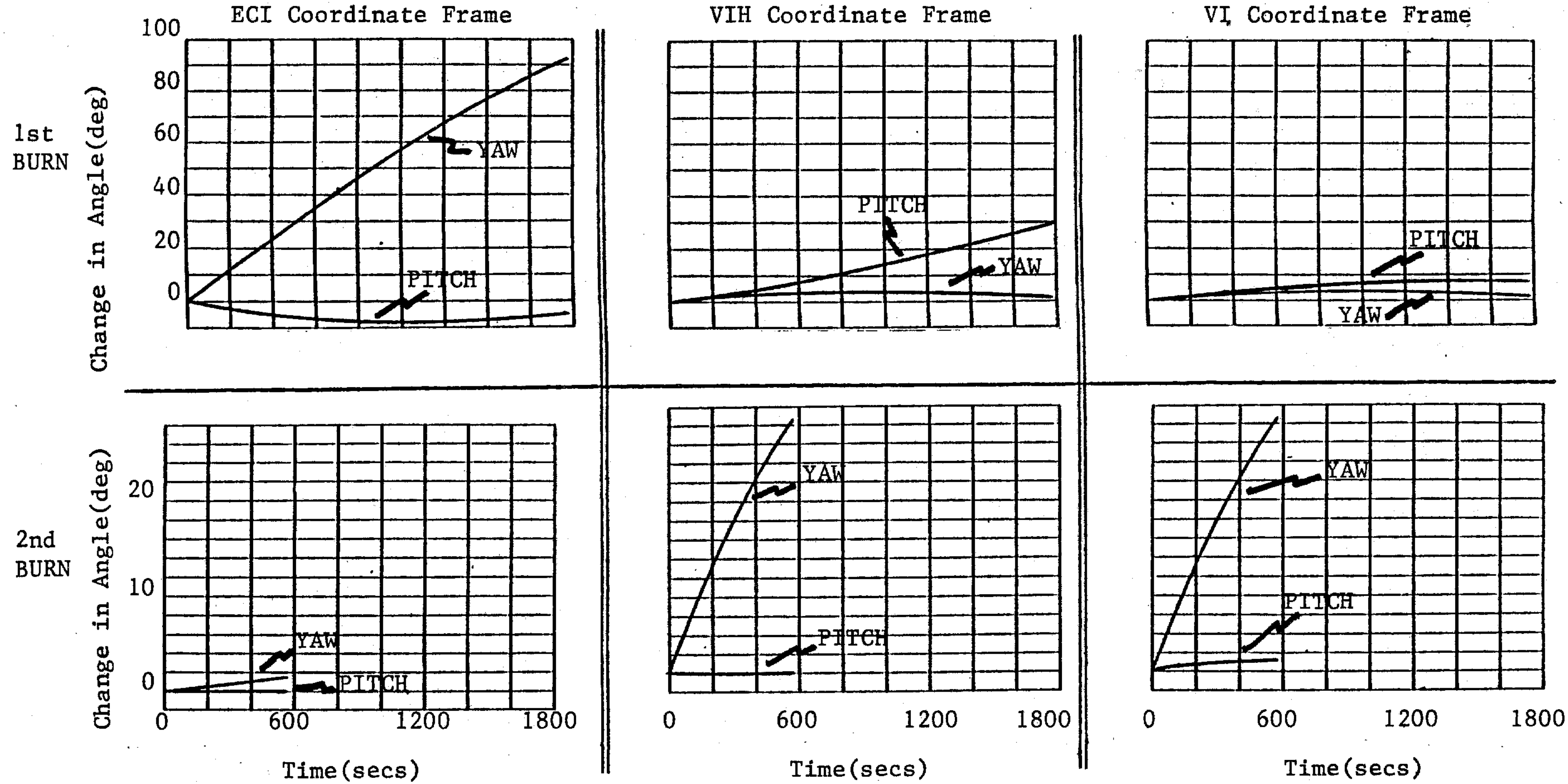

Figure 13. Changes in Thrust Pointing Angles for Transfer to 63.4 Degree Inclined, 300 nmi Altitude Circular Orbit

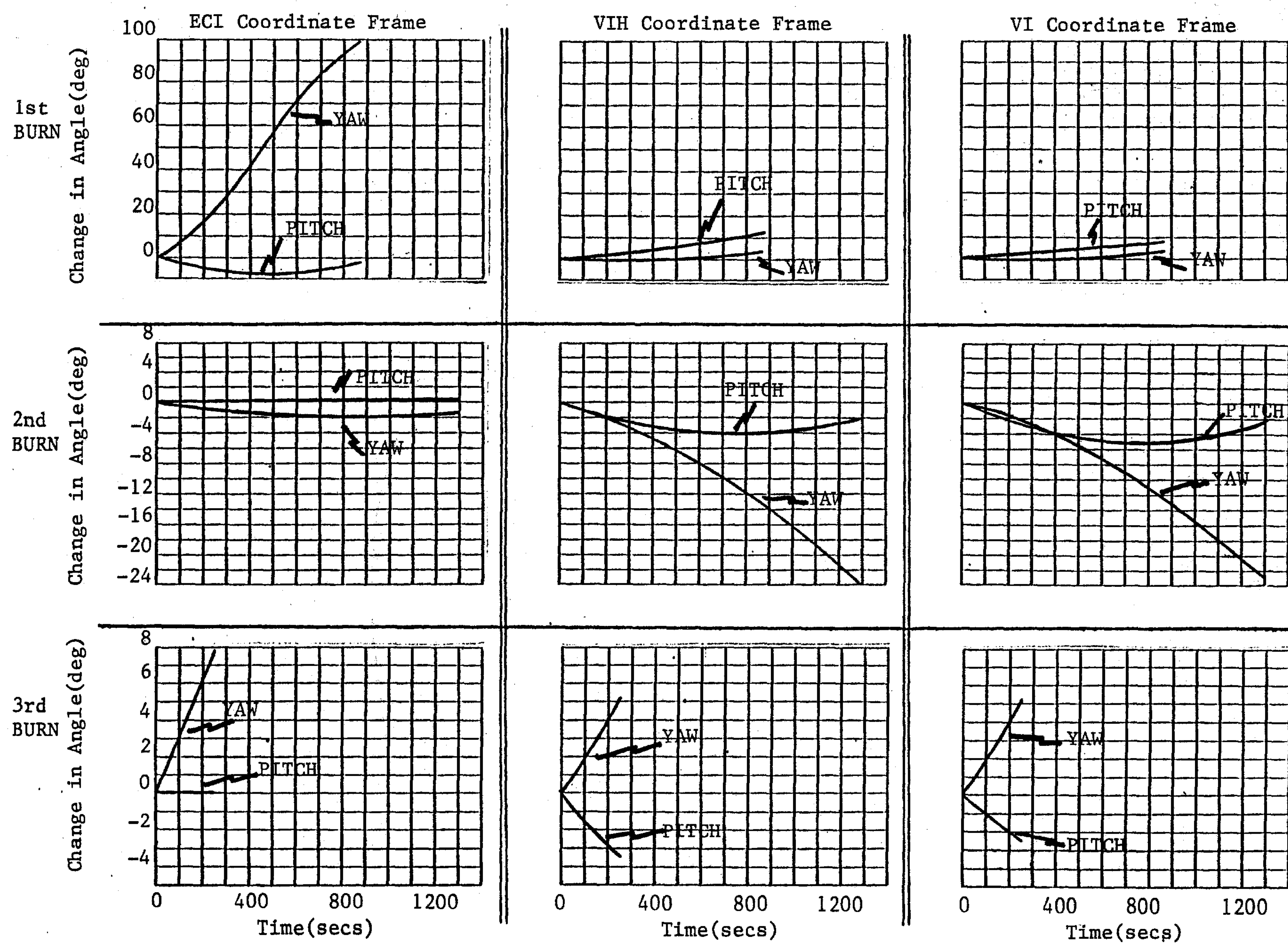

Figure 14. Changes in Thrust Pointing Angles for Transfer to 300 nmi Perigee Altitude Molniya Orbit

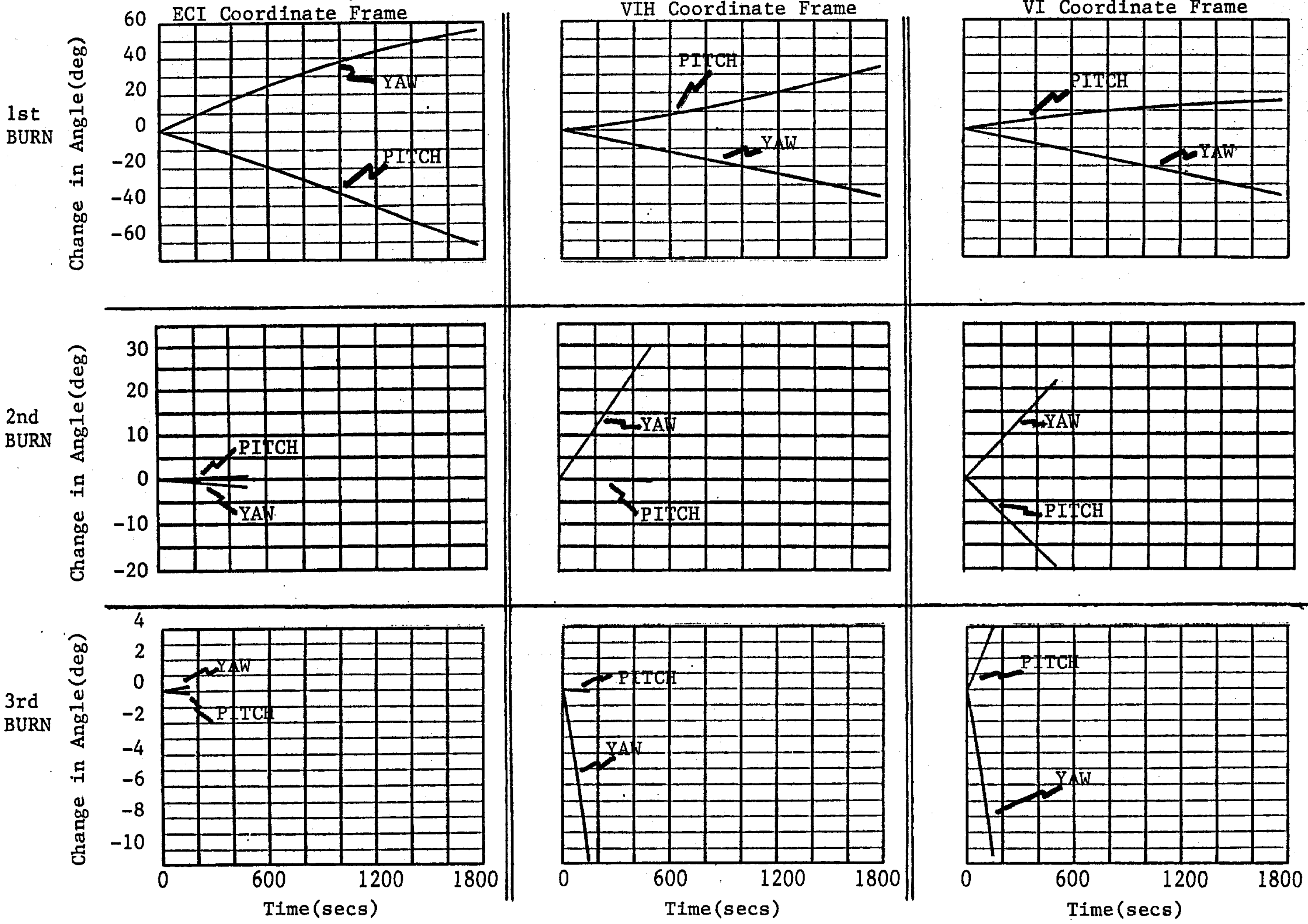

Inspection of Tables 9 to 13 and 22 to 26 reveals that the first and third burns of the transfers to the 63.4 degree inclined orbits can be classified mainly as orbit size changing burns, while the second burns of these transfers can be classified mainly as orbit plane changing burns. Similarly, Table 3 reveals that the first burn of the transfer to geosynchronous orbit is an orbit size changing burn while the second burn changes both orbit size and plane.

Correlating these classifications with the plots of Figures 12 to 14 reveals the following three characteristics:

1. for orbit size changing perigee burns, the pointing angles have the smallest variation when expressed in the VI coordinate frame, i.e., the thrust vector remains relatively fixed with respect to the inertial velocity vector;
2. for orbit size changing apogee burns, the pitch pointing angle has the smallest variation when expressed in the VIH coordinate frame, i.e., the thrust vector remains relatively fixed with respect to the local horizontal plane;
3. for orbit plane changing burns, the pointing angles have the smallest and most linear variation when expressed in the ECI coordinate frame, i.e., the thrust vector remains relatively fixed with respect to the inertial frame.

These results basically agree with those of Bartholomew-Biggs [14], who showed that use of linearly varying pointing angles in the VIH frame give near optimal performance. However, better performance might have been obtained by Bartholomew-Biggs if the ECI or VI frame had been used for some of the burns. Kaplan and Yang [15] reported that inertially fixed burns always give large velocity losses and that time varying pointing angles give the optimum performance. Kaplan and Yang did not state if this variation of the angles with time was linear, but this seems implied. They also did not define the coordinate system for their pointing angles. In spite of their omissions, the present study certainly confirms their assertion that time varying angles are better than inertially fixed angles. However, it is not clear that use of inertially fixed burns will always result in "large" velocity losses, especially if the burn is used to change the orbit plane. Exception is also taken to Kaplan and Yang's use of the word "optimum", since no information is given with regard to the coordinate frames or optimization procedures and criteria used to obtain their results.

Chapter 5

CONCLUSIONS AND SUGGESTIONS FOR FURTHER STUDY

5.1 CONCLUSIONS

The number and variety of orbit transfer problems which have been solved indicate that the HNLP method is a very effective method for solving optimal orbit transfer problems. The method is very simple to implement and formulate. All that is required is the system of algebraic-differential equations which constitutes the optimal control problem, an integration scheme, and an NLP algorithm. The formulation of the transversality functions is not required.

The use of the switch times as optimization variables and the zeroes of the switching function as constraints greatly aided the optimization process. By formulating the problem this way, the possibility of flying "wild" trajectories (which could happen if the switching function was used to determine when to burn and coast) during the optimization process is removed.

Based on the solutions obtained in this study, it appears that in general, an optimal orbit transfer consists of either three or two burns, depending not only on the size and orientation of the final orbit, but also on the magnitude of the thrust level. It was also found that the optimality of the solutions could be maintained only if the thrust level remained above a certain lower bound. Below this lower bound the positivity of the switching function during the first burn could not be maintained.

The results show that a high to low altitude transfer between two orbits is more fuel efficient than a low to high altitude transfer between the same two orbits and that an acceleration-limited transfer is more fuel efficient than a thrust-limited transfer having the same maximum acceleration. A general conclusion to be drawn from these results is that the length of a burn arc is apparently a more fundamental measure of finite burn loss than is the thrust or acceleration level.

The results also revealed that the finite burn solutions maintained a geometric similarity to the impulsive solutions. The locations of the burns and their effects on the transfer orbits were generally independent of the thrust level.

The analysis of the thrust pointing angles leads to the conclusion that the magnitude and time linearity of the change in the angles is dependent on the choice of coordinate frame used to represent these angles. In general, use of the ECI coordinate frame for orbit plane changing burns and VI or VIH coordinate frame for orbit size changing burns will result in the smallest and most linear time variation of the pointing angles.

5.2 SUGGESTIONS FOR FURTHER STUDY

Before this study was undertaken, the author was under the impression that as the thrust level was decreased to lower and lower levels, the burns of an optimal two or three burn solution would eventually coalesce into one burn, i.e., an optimal one burn solution would result. The results of this study indicate that apparently this cannot occur unless some of the optimality conditions are violated during the transition to a one burn solution. A more detailed investigation of this phenomenon is certainly one possible area for further study.

Other aspects of the orbit transfer problem to be investigated are the effects of much larger plane changes, the tradeoffs between multiple burns, transfer time, and finite burn loss, and comparisons of optimal two burn and three burn solutions for the same orbit transfers. An investigation could also be made of the performance penalties resulting from the use of simple steering strategies instead of the optimal steering strategy.

The generality of the HNLP method should allow it to be easily applied to other optimal control problems. The utility of the method for problems involving more complicated constraint functions would seem to be another fruitful area for investigation.

REFERENCES

1. Bell, D.J., "Optimal Space Trajectories - A Review of Published Work," Aeronautics Journal of Royal Aeronautical Society, Vol. 72, 1968, pp. 141-146.

2. Lawden, D.F., Optimal Trajectories for Space Navigation, Butterworth & Co. (Publishers) Ltd., London, 1963.

3. Betts, J.T., "Optimal Three-Burn Orbit Transfer," AIAA Journal, Vol. 15, No. 6, 1977, pp. 861-864.

4. Brusch, R.G., "Constrained Impulsive Trajectory Optimization for Orbit-to-Orbit Transfer," Journal of Guidance and Control, Vol. 2, No. 3, 1979, pp. 204-212.

5. Kechichian, J., "Optimal Transfer Between Close Near-Circular Orbits," IAF Paper 81-338, 32nd International Astronautical Congress, Rome, Italy, September, 1981.

6. Brusch, R.G. and Vincent, T.L., "Low-Thrust, Minimum Fuel, Orbital Transfers," Astronautica Acta, Vol. 16, No. 2, 1971, pp. 65-73.

7. Jasper, T.P., "Low-Thrust Trajectory Analysis for the Geosynchronous Mission." AIAA Paper 73-1072, AIAA 10th Electric Propulsion Conference, Lake Tahoe, Nevada, November, 1973.

8. Edelbaum, T.N., Sackett, L.L., Malchow, H.L., "Optimal Low Thrust Geocentric Transfer, "AIAA Paper 73-1074, AIAA 10th Electric Propulsion Conference, Lake Tahoe, Nevada, November, 1973.

9. Anderson, G.M. and Smith, E.A., "A Combined Gradient/Neighboring Extremal Algorithm for the Calculation of Optimal Transfer Trajectories between Noncoplanar Orbits Using a Constant Low Thrust Rocket," The Journal of the Astronatical Sciences, Vol. 23, No. 3, 1975, pp. 225-239.

10. Wood, L.J., "Comment on 'Application of the Conjugate Gradient Method to a Problem on Minimum Time Orbit Transfer'," IEEE Transactions on Aerospace and Electronic Systems, Vol. AES-13, No. 4, 1977, pp. 388-390.

11. Hersom, S.E., Dixon, L.C.W., Bartholomew-Biggs, M.C., and Pocha, J.J., "The Optimisation of Spacecraft Trajectories," H.S.D. Report TP 7633, Hawker Siddeley Dynamics Limited, Hatfield, England, 1977.

12. Bartholomew-Biggs, M.C., "The Optimisation of Spacecraft Orbital Manoeuvres Part II: Using Pontryagin's Maximum Principle," Numerical Optimisation of Dynamic Systems," Dixon, L.C.W. and Szego, G.P., (Editors), North-Holland Publishing Company, Amsterdam, 1980, pp. 49-74.

13. Redding, D. and Breakwell, J.V., "Optimal Low-Thrust Transfers to Synchronous Orbit," AAS Paper 81-130, AAS/AIAA Astrodynamics Specialist Conference, Lake Tahoe, Nevada, August, 1981.

14. Bartholomew-Biggs, M.C., "The Optimisation of Spacecraft Orbital Manoeuvres Part I: Linearly Varying Thrust Angles," Numerical Optimisation of Dynamic Systems, Dixon, L.C.W. and Szego, G.P. (Editors), North-Holland Publishing Company, Amsterdam, 1980, pp. 29-48.

15. Kaplan, M.H. and Yang, W., "Finite Burn Effects on Ascent Stage Performance," The Journal of the Astronautical Sciences, Vol. 30, No. 4, 1982, pp. 403-414.

16. Schappelle, R.H. and Brusch, R.G., "The Automation of Transversality Conditions," Optimal Control Applications & Methods, Vol. 1, 1980, pp. 93-98.

17. Bell, D.J. and Jacobson, D.H., Singular Optimal Control Problems, Academic Press, New York, 1975.

18. Bryson, A.E., and Ho, Y.C., Applied Optimal Control, Hemisphere Publishing Corp., Washington, D.C., 1975.

19. Kelley, H.J., "Singular Extremals in Lawden's Problem of Optimal Rocket Flight," AIAA Journal, Vol. 1, No. 7, 1963, pp. 1578-1580.

20. Pines, S., "Constants of the Motion for Optimum Thrust Trajectories in a Central Force Field," AIAA Journal, Vol. 2, No. 11, 1964, pp. 2010-2014.

21. Robbins, H.M., "Optimality of Intermediate-Thrust Arcs of Rocket Trajectories," AIAA Journal, Vol. 3, No. 6, 1965, pp. 1094-1098.

22. Bell, D.J., "The Non-Optimality of Lawden's Spiral," Astronautica Acta, Vol. 16, No. 6, 1971, pp. 317-324.

23. Archenti, A.R. and Vinh, N.X., "Intermediate-Thrust Arcs and Their Optimality in a Central, Time-Invariant Force Field," Journal of Optimization Theory and Applications, Vol. 11, No. 3, 1973, pp. 293-304.

24. Teschner, W., "Optimality of Intermediate-Thrust Arcs in Rotating Potential Force Fields," IAF Paper 79-185, 30th International Astronautical Congress, Munich, F.R.G., September, 1979.

25. Teschner, W., "Optimum Thrust Trajectories in General Central Force Fields," Journal of Guidance and Control, Vol. 2, No. 6, 1979, pp. 517-521.

26. McDanell, J.P. and Powers, W.F., "New Jacobi-Type Necessary and Sufficient Conditions for Singular Optimization Problems," AIAA Journal, Vol. 8, No. 8, 1970, pp. 1416-1420.

27. McDanell, J.P. and Powers, W.F., "Necessary Conditions for Joining Optimal Singular and Nonsingular Subarcs," SIAM J. Control, Vol. 9, No. 2, 1971, pp. 161-173.

28. Breakwell, J.V. and Dixon, J.F., "Minimum-Fuel Rocket Trajectories Involving Intermediate-Thrust Arcs," Journal of Optimization Theory and Applications, Vol. 17, No. 5/6, 1975, pp. 465-479.

29. Bershchanskii, Y.M., "Fusing of Singular and Nonsingular Parts of Optimal Control," Deterministic Systems, Plenum Publishing Corp., New York, 1979, Translated from Avtomatika i Telemekhanika, No. 3, 1979, pp. 5-11.

30. Blank, D. and Shinar, J., "Efficient Combinations of Numerical Techniques Applied for Aircraft Turning Performance Optimization," Journal of Guidance and Control, Vol. 5, No. 2, 1982, pp. 124-130.

31. Dixon, L.C.W. and Biggs, M.C., "The Advantages of Adjoint-Control Transformations When Determining Optimal Trajectories by Pontryagin's Maximum Principle," Aeronautical Journal, March, 1972, pp. 169-174.

32. Birta, L.G. and Trushel, P.J., "An Optimal Control Algorithm Using the Davidon-Fletcher-Powell Method with the Fibonacci Search, "AIChE Journal, Vol. 16, No. 3, 1970, pp. 363-368.

33. Vinh, N.X., "Integration of the Primer Vector in a Central Force Field," Journal of Optimization Theory and Applications, Vol. 9, No. 1, 1972, pp. 51-58.

34. Betts, J.T., "A Nonlinear Programming Algorithm Which Does Not Require Derivatives," Submitted for Publication in Journal of Optimization Theory and Applications, 1983.

35. Austin, R.E., Cruz, M.I. and French, J.R., "System Design Concepts and Requirements for Aeroassisted Orbital Transfer Vehicles," AIAA Paper 82-1379, AIAA 9th Atmospheric Flight Mechanics Conference, San Diego, California, August, 1982.